

**UNIVERSIDADE ESTADUAL PAULISTA - UNESP
FACULDADE DE CIÊNCIAS AGRÁRIAS E VETERINÁRIAS
CÂMPUS DE JABOTICABAL**

***EX VIVO* TORSIONAL PROPERTIES OF THE TARGON® VET
NAIL SYSTEM IN CANINE FEMURS: COMPARISON WITH
THE 2.4 mm LC-DCP® PLATE**

**Aline Schafrum Macedo
Médica Veterinária**

2015

**UNIVERSIDADE ESTADUAL PAULISTA - UNESP
FACULDADE DE CIÊNCIAS AGRÁRIAS E VETERINÁRIAS
CÂMPUS DE JABOTICABAL**

***EX VIVO* TORSIONAL PROPERTIES OF THE TARGON® VET
NAIL SYSTEM IN CANINE FEMURS: COMPARISON WITH
THE 2.4 mm LC-DCP® PLATE**

Aline Schafrum Macedo

Orientador: Prof. Dr. Bruno Watanabe Minto

Dissertação apresentada à Faculdade de Ciências Agrárias e Veterinárias – Unesp, Campus de Jaboticabal, como parte das exigências para obtenção do título de Mestre em Cirurgia Veterinária.

2015

M141e Macedo, Aline Schafrum
Ex vivo torsional properties of the Targon® Vet Nail System in canine femurs : comparison with the 2.4 mm LC-DCP® plate / Aline Schafrum Macedo. -- Jaboticabal, 2015
xi, 66 f. : il. ; 29 cm

Dissertação (mestrado) - Universidade Estadual Paulista, Faculdade de Ciências Agrárias e Veterinárias, 2015

Orientador: Bruno Watanabe Minto

Banca examinadora: André Escobar, André Luis Selmi

Bibliografia

1. Biomechanics 2. Dogs 3. Fracture fixation. I. Título. II. Jaboticabal-Faculdade de Ciências Agrárias e Veterinárias.

CDU 619:616.718.4:636.7

CERTIFICADO DE APROVAÇÃO


TÍTULO: ex vivo TORSIONAL PROPERTIES OF THE TARGON VET NAIL SYSTEM IN CANINE FEMURS: COMPARISON WITH THE 2.4 mm LC-DCP PLATE


AUTORA: ALINE SCHAFRUM MACEDO

ORIENTADOR: Prof. Dr. BRUNO WATANABE MINTO

Aprovada como parte das exigências para obtenção do Título de MESTRE EM CIRURGIA VETERINÁRIA, pela Comissão Examinadora:


Prof. Dr. BRUNO WATANABE MINTO
Departamento de Clínica e Cirurgia Veterinária / Faculdade de Ciências Agrárias e Veterinárias de Jaboticabal


Prof. Dr. ANDRÉ ESCOBAR
Departamento de Clínica e Cirurgia Veterinária / Faculdade de Ciências Agrárias e Veterinárias de Jaboticabal


Prof. Dr. ANDRÉ LUIS SELMI
Universidade Anhembi Morumbi / São Paulo/SP

Data da realização: 06 de novembro de 2015.

DADOS CURRICULARES DA AUTORA

ALINE SCHAFRUM MACEDO, nascida na cidade de Curitiba, Estado do Paraná, em 03 de Março de 1985. Graduou-se em Medicina Veterinária em dezembro de 2009, pela Faculdade de Medicina Veterinária da Universidade Federal do Paraná – UFPR – Campus de Curitiba com o trabalho intitulado “Tarsometatarsal partial arthrodesis with use of circular skeletal fixator on a dog”. Concluiu o Programa de Residência em Clínica e Cirurgia Veterinária da Universidade Federal do Rio Grande do Sul – UFRGS na turma 2010-2012 com o trabalho intitulado “Hemangiosarcoma in the Radius of a Dog Treated by Limb-sparing Surgery”. Participou do Programa de Fellowship da AO Foundation na University of Guelph (Guelph, Ontario, Canada) em 2013. Ingressou no Programa de Pós-Graduação em Cirurgia Veterinária em Março de 2014, sob orientação do Prof. Dr. Bruno Watanabe Minto em parceria com a University of Guelph sob orientação do Prof. Noel M. M. Moens. É integrante do corpo clínico de atendimento do Serviço de Ortopedia e Neurologia do Hospital Veterinário “Governador Laudo Natel”, da UNESP Jaboticabal.

Epígrafe

“Viver é sempre dizer aos outros
Que eles são importantes.
Que nós os amamos.
Porque um dia eles se vão
E ficaremos com a impressão
De que não os amamos o suficiente.”

Chico Xavier

Dedicatória

Aos meus pais,
Ruben Cesar e Carmen Lucia,

A quem devo tudo o que sou e onde cheguei.
Com eternas saudades.

A minha amada vó,
Tita,

Pela paciência, ensinamentos e amor.
Obrigada por tudo.

Ao meu querido,
Renato

Por todo amor, carinho, paciência, cuidado e dedicação
todos esses anos.

AGRADECIMENTOS

Agradeço a Deus, pela minha vida, por todas as oportunidades que me foram oferecidas, pelas pessoas que em meu caminho adentraram e por tudo que ainda me é reservado.

Agradeço aos meus pais pelo amor recebido no tempo que estivemos juntos e por terem me proporcionado uma vida tão boa.

À minha avó Tita por toda a paciência, amor e ajuda e pelos ótimos momentos que sempre compartilhamos.

Ao meu namorado, Renato Barbosa Silva, por todo amor, paciência, ajuda, companheirismo e maravilhosos momentos que tivemos durante toda a nossa caminhada.

À família Barbosa Silva que me acolheu e hoje tenho como minha.

Ao meu orientador Prof. Dr. Bruno Watanabe Minto pela oportunidade, tempo dispendido e por contribuir para meu crescimento pessoal e profissional.

Ao meu co-orientador Prof. Noel Moens pela confiança em mim depositada, ajuda na elaboração e execução deste projeto, orientação durante toda a minha permanência no Canadá, pela imensurável oportunidade e pelo seu apoio.

Ao engenheiro Prof. Dr. John Runciman pelo apoio na elaboração e execução do projeto, sem o qual não teria sido possível a realização do trabalho.

Aos técnicos da Universidade de Guelph: Carly Fennel, Amanda Hathway, Nicole Kudo, Steve Wilson por toda a ajuda na execução do projeto.

Ao Prof. Thomas Gibson da Universidade de Guelph pela ajuda na elaboração e execução do projeto e por ter emprestado todo o instrumental necessário a realização do mesmo.

Ao Professor Dr. Antônio Felipe Paulino de Figueiredo Wouk, por todo o incentivo durante todos esses anos, por ser essa pessoa maravilhosa, exemplo de perseverança, além de um grande amigo.

Ao Professor Dr. Alexandre Schmaedecke, sem o qual sequer teria tido conhecimento da Ortopedia Veterinária e pela ajuda que me ofereceu todos esses anos.

Aos Professores Dr. Marcelo Meller Alievi e Dr. Afonso de Castro Beck por todo o maravilhoso tempo de residência, pelos ensinamentos e apoio durante momentos delicados.

A todos os amigos do serviço de Ortopedia e Neurologia da Unesp Jaboticabal pelo

companheirismo, ensinamentos e vivência nesse tempo em que estivemos juntos em Jaboticabal, especialmente às queridas amigas Fabrícia Filgueira, Arícia Sprada e Denise Chung, presentes do destino.

À minha amada amiga Isís dos Santos Dal-Bó por todo o apoio, incentivo, momentos hilários e incentivo a pesquisa.

Ao CNPq e CAPES, pela bolsa a mim concedida durante todo o Mestrado.

À AO Foundation pelo Fellowship concedido em 2013 que me trouxe a oportunidade de realizar esse trabalho.

À Fundação Pet Trust do Ontario Veterinary College pelo suporte financeiro concedido ao projeto.

À Pró-reitoria de Pesquisa da Unesp Jaboticabal pelo auxílio concedido para a realização da pesquisa no exterior.

Agradeço também a todos os profissionais que me inspiraram e incentivaram até hoje, contribuindo com conhecimento nos diversos estágios e cursos que fiz durante a minha graduação.

Agradeço principalmente aos animais por fazerem parte do meu processo de aprendizado e da paixão que escolhi por profissão.

SUMMARY

RESUMO	iv
ABSTRACT	v
LIST OF FIGURES	vi
LIST OF TABLES	x
LIST OF ABBREVIATIONS	xi
1. INTRODUCTION	1
2. LITERATURE REVIEW	3
2.1 Bone.....	3
2.1.1 one Composition	3
2.1.2 omechanical properties.....	4
2.2 Mechanical Testing	7
2.3 Femoral fractures	9
2.4 Fracture healing and Internal Fixation.....	10
2.5 Interlocking Nails.....	14
2.6 Targon® Vet Nail System.....	20
3. PURPOSE	24
3.1 Specific Goals	24
3.2 Hypotheses.....	24
4. MATERIAL AND METHODS	25
4.1 Ethic Considerations	25
4.2 Specimen collection	25
4.3 Implants	27
4.4 Specimen preparation.....	31
4.5 Biomechanical analysis	38
4.6 Statistical analysis.....	43
5. RESULTS	44
5.1 Specimens	44
5.2 Torsion tests.....	45
5.2.1 ycllic loading	46
5.2.2 Load to failure	47

6. DISCUSSION53
7. CONCLUSION56
8. REFERENCES57



UNIVERSIDADE ESTADUAL PAULISTA
CÂMPUS DE JABOTICABAL
Departamento de Clínica e Cirurgia Veterinária



CEUA – COMISSÃO DE ÉTICA NO USO DE ANIMAIS

CERTIFICADO

We certify that the Protocol nº 009278/14 of the research study entitled "**Ex vivo torsional properties of the Targon Vet™ Nail System in feline femurs: Effect of hole size and location**" under the responsibility of Prof. Dr. Bruno Watanabe Minto is in accordance to the Ethical Principles in Animal Experimentation adopted by the National Council for Animal Experiments Control (CONCEA) and was approved by the ETHICS IN ANIMAL USE COMMITTEE (CEUA) at a regular meeting of June 6, 2014 .

Jaboticabal, 06 de junho de 2014


Prof.ª Dr.ª Paola Castro Moraes
Coordenadora – CEUA

PROPRIEDADES TORSIONAIS *EX VIVO* DO SISTEMA DE HASTE TARGON® VET EM FÊMURES CANINOS: COMPARAÇÃO COM A PLACA LC-DCP® DE 2,4 mm

RESUMO – O objetivo desse trabalho foi avaliar a estabilidade torsional do sistema *Targon Vet Nail* (TVS) de 2,5 mm em fêmures de cães pequenos e estudar o efeito de diferentes localizações dos bolts na força torsional das construções, comparadas a placas de baixo contato *Low Contact – Dynamic Compression Plate* (LC-DCP®) de 2,4 mm. Trinta e seis fêmures foram obtidos de cadáveres frescos de cães pequenos e alocados em 3 grupos (n = 12), assegurando distribuição de comprimento do osso igual entre os grupos. Em todos os ossos, o ponto 1 mm abaixo do trocânter menor e outro 1 mm acima das fabelas foram marcados e uma osteotomia transversa foi realizada equidistante a essas marcações, na diáfise. No grupo 1, o osso foi fixado com o TVS de 2,5 mm com os parafusos aplicados nessas marcas pré-identificadas, deixando um espaço de 2 mm entre os fragmentos. No grupo 2, o sistema TVS também foi utilizado, mas o parafuso proximal foi colocado num local equidistante entre a marcação e a osteotomia proximal, resultando em uma distância entre os parafusos 25% mais curta. No grupo 3, placas LC-DCP® de 2,4 mm e 7 orifícios foram aplicadas à face lateral dos ossos. Todas as construções foram testadas de forma não destrutiva a uma taxa de 1°/s sob torque controlado de mais e menos 0,57 Nm durante 10 ciclos. O teste cíclico foi seguido por uma torção aguda até ocorrer falha. O último dos 10 ciclos foi usado para medir a deformação sob carga não-destrutiva. A rigidez e torque até falha foram medidos a partir das curvas finais de torque-deformação. O limite elástico foi definido como uma deformação de 1° para além do comportamento linear esperado das construções. Todos os resultados foram testados quanto à normalidade e comparados utilizando análise de variância e teste *post hoc* de Tukey. Valores de P < 0,05 foram considerados significativos. Torque máximo +/- desvio padrão foi 0,806 +/- 0,183 e 0,805 +/- 0,093 Nm para os grupos 1 e 2 e 1,737 +/- 0,461 Nm para o grupo 3. A rigidez foi 0,05 +/- 0,01; 0,05 +/- 0,007 e 0,14 +/- 0,015 Nm/° para os grupos 1 a 3, respectivamente. Deslocamento sob carga cíclica foi de 16,6° +/- 2,5°; 15,6° +/- 2,1° e 7,8° +/- 1,06°, respectivamente. Não houve diferença significativa para qualquer um dos parâmetros entre os grupos 1 e 2. No entanto houve diferença significativa em todos os parâmetros analisados entre o grupo 3 e os grupos 1 e 2. Não foi detectada nenhuma interação entre a distância entre os parafusos e o diâmetro do osso em qualquer um dos parâmetros em qualquer dos grupos. A falta de interação entre a distância entre o parafuso e a rigidez foi inesperada e sugere que a rigidez do sistema é mais uma função do mecanismo de bloqueio dos parafusos na haste, em vez das propriedades da própria haste. Fato também sugerido pelo grande deslocamento observado sob cargas cíclicas e as marcas alongadas deixadas mecanismo de bloqueio dos parafusos da haste sugerindo deslizamento de um dos dois parafusos. As outras forças atuantes no animal vivo devem ser testadas *in vitro* para que recomendações sobre a utilização em casos clínicos sejam possíveis.

Palavras-chave: Biomecânica, cães, cirurgia veterinária, fixação de fratura, ortopedia

EX VIVO TORSIONAL PROPERTIES OF THE TARGON® VET NAIL SYSTEM IN CANINE FEMURS: COMPARISON WITH THE 2.4 mm LC-DCP® PLATE

ABSTRACT – The purpose of this study was to evaluate the torsional stability of the Targon® Vet Nail System (TVS) in small canine femurs and to study the effect of different bolt locations on the torsional strength of the constructs compared to 2.4 mm Low Contact – Dynamic Compression Plates (LC-DCP®). Thirty-six femurs were harvested from fresh small dog cadavers and allocated to 3 groups (n=12) ensuring equal bone length distribution between groups. In all bones, points 1 mm below the lesser trochanter and 1 mm above the fabellae were marked and a transverse osteotomy was performed in the middle. In group 1, the bone was fixed with the 2.5 mm TVS with the bolts applied at those pre-identified marks, leaving a 2 mm gap between fragments. In group 2, the TVS was also used but the proximal bolt was placed in a location equidistant between the proximal mark and the osteotomy, resulting in a 25% shorter inter-bolt distance. In group 3, 7-hole 2.4 mm LC-DCP® plates were applied to the lateral aspect of the bones. All constructs were tested non-destructively at a rate of 1°/sec under load control between a torque of plus and minus 0.57 Nm for 10 cycles. Cyclic loading was followed by an acute torsion to failure. The last of the 10 cycles was used to measure the deformation under non-destructive load. The stiffness and torque to failure of the constructs were measured from the final torque-deformation curves. Yield point was defined as a 1° deformation beyond the expected linear behavior of the constructs. All results were tested for normality and compared using ANOVA and Tukey post hoc tests. P values < 0.05 were considered significant. Torque at yield was 0.806 +/- 0.183 and 0.805 +/- 0.093 Nm for groups 1 and 2 and 1.737 +/- 0.461 Nm for group 3. Stiffness was 0.05 +/- 0.01; 0.05 +/- 0.007 and 0.14 +/- 0.015 Nm/° for groups 1 to 3 respectively. Displacement under cyclic loading was 16.6° +/- 2.5°; 15.6° +/- 2.1° and 7.8° +/- 1.06° respectively. There was no significant difference for any of the parameters between groups 1 and 2. All parameters examined were however significantly different between group 3 and groups 1 and 2. There was no interaction detected between bolt distance and bone diameter for any of the parameters in any of the groups. The lack of interaction between bolt distance and stiffness was unexpected. It suggests that the system's stiffness is more a function of the bolt gripping mechanism on the nail rather than the properties of the rod itself. The latter is also supported by the large displacement observed under cyclic loading and the elongated marks left by the locking mechanism of the bolts on the rod suggesting slippage of one of the two bolts. Other forces that act on the living animal should be measured *in vitro* so that recommendations can be made for clinical tests.

Keywords: Biomechanics, dogs, fracture fixation, orthopaedics, veterinary surgery

LIST OF FIGURES

- Figure 1 – . Load-deformation curve demonstrating elastic and plastic regions of bone. Young's modulus (E) equals the slope. The vertical line represents stress applied, and the horizontal line represents strain. Adapted from Sharir et al., 2008.....6
- Figure 2 – Targon® Vet Nail System (TVS). A) Schematic drawing of the TVS applied to a feline femur. B) Schematic drawing of the locking mechanism. The fixing screw fits inside the bolt and locks the construct with the nail. C) Picture of two locking bolts (blue arrows) and one fixing screw (black arrow). Source: B. Braun Vet Care GmbH, 201521
- Figure 3 – A) Craniocaudal (cr-ca) radiographic view of a right canine femur. B) Canine right femur after softer tissues removal. Guelph, 2014.....26
- Figure 4 – A) Targon® Vet Nail System (TVS) implants. Intramedullary nail with 2.5 mm of diameter (white arrow). Locking screws (red arrow) with lengths between 16 and 22 mm and fixing screws (black arrow) used to lock the TVS construct. B) Locking screw with on part of 2.8 mm of outer diameter (red arrow) and the thicker part with outer diameter of 4.8 mm (black arrow). C) Fixing screw with 3 mm of outer diameter. Guelph, 201428
- Figure 5 – A) TVS instrument set box one: drill bits (red arrow), drill guides (green arrow) and depth gauge (yellow arrow). B) TVS instrument set two, with pin cutter (light blue arrow), torquimeter (yellow arrow) and screwdriver (pink arrow). C) TVS implants box with 2.5 mm (red arrow) and 3 mm implants (yellow arrow). D) 2.5 mm implants on detail with nails (yellow arrow) and screws (red arrow). Guelph, 201429
- Figure 6 – A) TVS instrument set box one: drill bits (red arrow), drill guides (green arrow) and depth gauge (yellow arrow). B) TVS instrument set two, with pin cutter (light blue arrow), torquimeter (yellow arrow) and screwdriver (pink arrow). C) TVS implants box with 2.5 mm (red arrow) and 3 mm implants (yellow arrow). D) 2.5 mm implants on detail with nails (yellow arrow) and screws (red arrow). Guelph, 201430
- Figure 7 – A) Canine right femur with the points immediately below the lesser trochanter and just above the fabellae marked (red dots).

- B) After the points were marked, the distance between them was measured (X), and the midpoint was defined as the osteotomy line. Guelph, 2014x 32
- Figure 8 – A) Picture of centering drill sleeve. B) Drawing of positioning the drill sleeve to drill the cis-cortex hole. C) Picture of the 4 mm drill bit. D) Drawing of the drilling procedure of the cis-cortex. Source: B. Braun Vet Care GmbH, 2015 32
- Figure 9 – A) Picture of drill sleeve with internal diameter of 2.5 mm that fits the cis-cortex hole. B) Picture of a 2.5 mm drill bit. C) Drawing of the sleeve being inserted through the cis-cortex hole and drilling of the trans-cortex by the 2.5 mm drill bit. Source: B. Braun Vet Care GmbH, 2015 33
- Figure 10 – A) Picture of a canine right femur from Group 1. Note the osteotomy line crossed in the mid distance between the two holes drilled. B) Picture of the same femur having the cis-cortex tapped. Guelph, 2014..... 33
- Figure 11 – A) Picture of a canine right femur from group 1 with both screws in position and the intramedullary nail inserted. B) Picture of the same femur after the tip of the nail that remained outside of the bone was cut. Fixing screws were inserted and locked by use of a special 1.8 Nm torque screwdriver (blue instrument). Guelph, 2014..... 34
- Figure 12 – A) Canine right femur from group 2. After the points were marked, the distance between them was measured (X), and the midpoint was defined as the osteotomy line. The midpoint between the first landmark and the osteotomy line was set to be the hole for the proximal screw (black dot). B) Canine right femur from group 2 with TVS in place. Guelph, 2014 35
- Figure 13 – Canine left femur from Group 3 with a 7-hole LC-DCP® plate laterally applied with the middle hole left empty at the osteotomy level (red arrow). A) Lateral aspect. B) Cranial aspect. Guelph, 2014 36
- Figure 14 – Craniocaudal radiographs used to ascertain correct positioning of the implants. A) Right specimen from group 1 (long nail) with the TVS in place. B) Right specimen from group 2 (short nail) with the TVS in place. C) Right specimen from group 3 with the plate and screws in position. Guelph, 2014 37
- Figure 15 – Latero-medial radiographs used to ascertain correct positioning of the implants. A) Right specimen from group 1 (long nail) with

- the TVS in place. B) Right specimen from group 2 (short nail) with the TVS in place. C) Right specimen from group 3 with the plate and screws in position. Guelph, 2014.....38
- Figure 16 – A) Steel cube of 2.5 x 2.5 X 2 cm used for positioning bones for potting. Duct tape was placed along the cube’s base to prevent the epoxy from leaking out of the cube. B) Epoxy resin West System 105/205 Epoxy Resin® with hardener. C) Custom-made potting fixture Note bones with the distal epiphyses embedded in epoxy resin (white arrow). Guelph, 2014.....39
- Figure 17 – Custom designed torsion jig with specimen from group 2 (short nail).Guelph, 201440
- Figure 18 – A) Torsion fixture attached to the Instron universal testing machine connected to a 0.5 kN load cell by a metal bar (yellow arrow), with bone sample ready for non-destructive cyclic load torsion test. B) Torsion wheel attached to a wire cable (red arrow) connected to the load cell by a block with pivots (blue arrow), for load to failure test. Guelph, 2014.....41
- Figure 19 – Torsion jig with an aluminium bar (white arrow) before test. Guelph, 2014.....42
- Figure 20– Schematic graph representing an example of the load/displacement curves for groups 1 and 2 (TVS nails) (light grey line), for group 3 (plates) (dark grey line) and the rigid steel bar (pink line) on cyclic tests. Guelph, 201446
- Figure 21 – Bar chart representing means and SD compliances of all groups. Group 1 (blue), group 2 (red) and group 3 (green). Guelph, 201447
- Figure 22 – Schematic graph representing examples of load/displacement curves of all groups: Group 1 (blue), group 2 (red) and group 3 (green).The grey line and dots indicate the yield point calculated by linear regression. Guelph, 201448
- Figure 23 – Bar chart representing means and SD for torque at yield of all groups. Group 1 (blue), group 2 (red) and group 3 (green). Guelph, 2014.....49
- Figure 24 – Bar chart representing means and SD for stiffness of all groups. Group 1 (blue), group 2 (red) and group 3 (green). Guelph, 201450
- Figure 25 – Implants retrieved after load to failure tests. A) A 2.4 mm LC-DCP® plate bent after test. B) A 2.5 mm nail with an elongated mark left by the locking mechanism of the bolts after the test

(red arrow). C) A 16 mm TVS bolt and fixing screw without any structural damage, retrieved after test. Guelph, 2014.....53

LIST OF TABLES

Table 1 – . Bone’s measurements. LesserT width = medullary width at the Lesser Trochanter landmark in mm. MidS width = medullary canal width at the midshaft landmark in mm. Fabellae width = medullary canal width on the imaginary point just above the Fabellae in mm. Guelph, 2014	44, 45
Table 2 – Mean +/- SD of bone’s measurements distribution between groups. LesserT width = medullary width at the Lesser Trochanter landmark in mm. MidS width = Medullary canal width at the midshaft landmark in mm. Fabellae width = Medullary canal width on the imaginary point just above the Fabellae in mm. Guelph, 2014	45
Table 3 – Comparison of means and standard deviations (SD) of all groups for compliance after cyclic loading test. Different letters show significant statistic difference on Tukey test at 5% confidence level. Guelph, 2014	47
Table 4 – Comparison of means and standard deviations (SD) of all groups for yield torque after load to failure test. Different letters show significant statistic difference on Tukey test at 5% confidence level. Guelph, 2014	49
Table 5 – Comparison of means and standard deviations (SD) of all groups for stiffness after load to failure test. Different letters show significant statistic difference on Tukey test at 5% confidence level. Guelph, 2014	50
Table 6 – Tests results of all groups. “Bolt dist” = distance between bolts for groups 1 and 2. For group 3 the distance considered was the length of the plates. “Stiff” = Torsional Stiffness, “Yield’ = Torque at Yield, “Compliance’ = Displacement under cyclic loading. Guelph, 2014	51
Table 7 – Mean +/- SD of all groups. “Bolt dist” = distance between bolts for groups 1 and 2. For group 3 the distance considered was the length of the plates. “Stiff” = Torsional Stiffness, “Yield’ = Torque at Yield, “Compliance’ = Displacement under cyclic loading. Different letters show significant statistic difference on Tukey test at 5% confidence level. Guelph, 2014	52

LIST OF ABBREVIATIONS

- AMI:** Area Moment of Inertia
- ANOVA:** Analysis of Variance
- AO:** Arbeitsgemeinschaft für Osteosynthesefragen
- ASIF:** Association for the Study of Internal Fixation
- Cr-ca:** Cranio-Caudal
- CRIF:** Clamp Rod Internal Fixation
- CT:** Computed Tomography
- IN:** Interlocking Nail
- INs:** Interlocking Nails
- J:** Polar Moment of Inertia
- LC-DCP:** Low Contact – Dynamic Compression Plate
- LN:** Long Nail
- M** - Meter
- MINO:** Minimally Invasive Nail Osteosynthesis
- MIO:** Minimally Invasive Osteosynthesis
- Mm** – Millimeters
- N** - Newton
- Nm:** Newton Meter
- OBDNT:** Open-but-do-not-touch technique
- ORIF:** Open Reduction and Internal Fixation
- PMI:** Polar Moment of Inertia
- R:** Maximum radial distance
- SD:** Standard Deviation
- SN:** Short Nail
- T:** Torque
- TVS:** Targon Vet Nail System

1. INTRODUCTION

Musculoskeletal injuries are very common in small animal practice and usually result in long bone fractures (LARIN et al., 2001). In order to obtain mechanical stability and allow early weight bearing besides rapid bone healing, internal fixation is recommended (ARON; JOHNSON; PALMER, 1995).

Although many different fixation methods can be used for repairing femoral fractures (LARIN et al., 2001; STIFFLER, 2004), Static Interlocking Nails (INs) have several advantages over other fixation systems. Their central intramedullary location, large sizes and locking capabilities distinguish them from most other implants (SCHANDELMAIER et al., 2000). Interlocking nails can be placed following the biological osteosynthesis principles with minimal surgical exposure (JOHNSON, 2003). There are few studies in small dogs and cats because their restricted intramedullary space turns the placement of interlocking nails challenging (DÍAZ-BERTRANA et al., 2005; DUELAND et al., 1999; LARIN et al., 2001).

A new device – Targon® Vet Nail System (TVS) has been recently adapted for veterinary purposes: it consists of a smaller intramedullary rod that fits into the long bones of small dogs and cats. The locking mechanism consists of locking bolts that can be positioned at the discretion of the surgeon to fit the individual patient. The locking mechanism of the TVS differs significantly from those of conventional nails. It consists of a bolt gripping the metal rod, as opposed to the bolt fitting inside a hole in the nail itself. It has only one nail size for every bone, with arbitrary number and direction of bolts. The TVS needs no aiming device or fluoroscopy and adjustments on length and rotation are possible after nail insertion (BRÜCKNER; UNGER; SPIES,

2014).

Biomechanical testing is primary for characterizing efficiency of different treatment modalities on bones and has great value to researchers and clinicians (ATHANASIOU et al., 2000; SHARIR; BARAK; SHAHAR, 2008). The TVS has not been extensively tried or tested. Limited biomechanical studies performed by the company (Aesculap-unpublished data) and by Brückner et al. (2014) are encouraging; however, significant questions regarding its safety and applications remain once the system had not yet been tested with whole bone under torsion forces so far

The purpose and goals of this research project was to evaluate the torsional stability of the locking mechanism in femurs of small dogs, to study the effect of different bolt locations on the torsional strength of the constructs and to compare it with Low Contact – Dynamic Compression Plates (LC-DCP®). We aimed to elucidate some of the biomechanical characteristics of the nail in torsion and to provide knowledge regarding the position of bolts on bone. The TVS is a device that requires minimal inventory and equipment compared to other nail systems. Because of its relative small size, it fits smaller animals, different from the current nail systems on the market. This new system could represent a viable option for the repair of comminuted long bone fractures in small dogs and cats.

2. LITERATURE REVIEW

2.1 Bone

The word bone can describe both the organ bone and the tissue (material) (SHARIR; BARAK; SHAHAR, 2008). Bones compose the framework of the body of every vertebrate animal. This specialized tissue has different functions within an animal's body including protection for internal organs, hematopoiesis and scaffolding for muscle attachments to allow strength and mobility (MARKEL et al., 1994; ROE, 1998).

2.1.1 Bone Composition

Bone is a heterogeneous specialized connective tissue composed of inorganic mineral substance (calcium phosphate hydroxyapatite), organic matrix (type I collagen fibrils, noncollagenous proteins, proteoglycans, phospholipids and water) and also blood vessels, nonosseous cells, nerve fibers and bone marrow with fundamental physiological roles (BONUCCI, 2000; SHARIR; BARAK; SHAHAR, 2008). Collagen fibrils and hydroxyapatite mineral matrix are the two components that most contribute to mechanical behavior (ROE, 1998). Structural and molecular integrity of the mineral reservoir is associated with stiffness whereas the collagen entanglement is responsible for post-yield and fracture properties (ZIOUPOS; CURREY; HAMER, 1999).

Macroscopically, bones are composed of cortical (compact) and cancellous (trabecular) tissue. The first consists of the hard outer shell composed of lamellae and provides stiffness. The latter is composed of trabeculae arranged as a porous network or loose mesh that allows blood vessel growth and energy absorbing ability. Long

bones have medullary cavities that store the marrow (BONUCCI, 2000).

2.1.2 Mechanical properties

Bone is a material with measurable characteristics such as hardness, resistance, moderate elasticity, and limited plasticity. It attenuates sonic or ultrasonic waves, dissipates energy and are ideal for standing and moving (BONUCCI, 2000; GIBSON et al., 2008). Cortical bone exhibits viscoelastic behavior, modifying its mechanical properties and deforming as a response to the forces the tissue is submitted to *in vivo* loading (AUTEFAGE, 2000; GIBSON et al., 2008). Osseous tissue has the ability to regenerate and repair itself, thus altering its morphology and those mechanical characteristics and exhibits piezoelectric properties (An et al. 2000). Bone is considered anisotropic, therefore its response to load depends on the direction on which the load is applied. Bone remodeling occurs according to Wolff's law - Osteoblasts lay down bone where needed and osteoclasts resorb where it is not needed in response to mechanical stresses placed on the osseous tissue (ROE, 1998).

Stress is defined as the load per unit area and strain is a tensor quantity that represents the fractional change in dimension (deformation) of a loaded body (SHARIR; BARAK; SHAHAR, 2008). It is possible to correlate the load suffered and the deformation caused by the exponential response curve generated called stress/strain curve (Figure 1). The curve is affected by material properties, geometry and structural morphology (AUTEFAGE, 2000; RAHN, 2002). Strain is the geometric change presented in response to a determined force (deformation per unit time) (AN et al., 2000). Constant applied stress and its gradual augmentation exhibits, at first, a

linear relation with strain; the material deforms elastically proportional to the tensile force and returns to its original form when the stress is removed. This linear relationship of elasticity is called Hooke's law (SHARIR; BARAK; SHAHAR, 2008).

In a second part, the curve is non-linear, and the strain lengthening becomes larger for the same load applied (AUTEFAGE, 2000; SHARIR; BARAK; SHAHAR, 2008). Once a particular point (yield point) is reached, any further increment in load results in a non-linear and irreversible (permanent) plastic deformation. If loading is continued, the mechanical strength limit is crossed, causing the bone to fail/fracture (AUTEFAGE, 2000).

The ratio between stress applied (σ) and resulting strain (ϵ) is the coefficient of proportionality represented by what is called Young's modulus (E) or modulus of elasticity, represented by the formula:

$$\sigma = E \cdot \epsilon$$

This modulus shows the material's stiffness and is represented by the slope (Figure 1) of the linear portion of the curve for normal loading (AUTEFAGE, 2000; SHARIR; BARAK; SHAHAR, 2008).

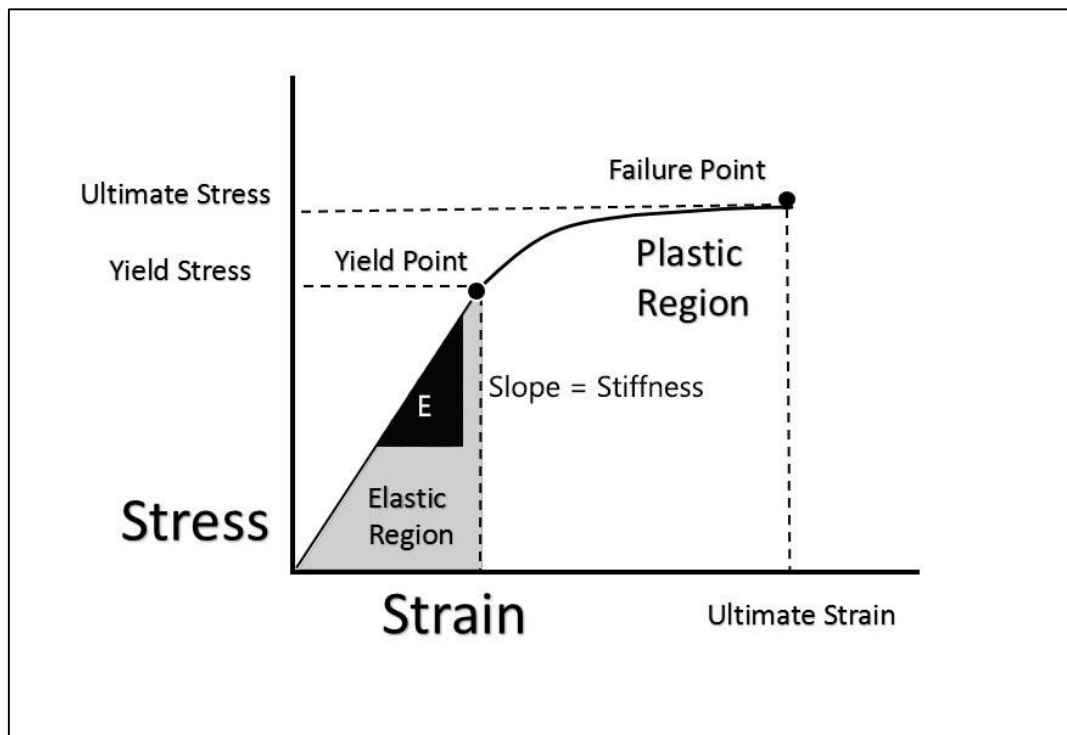


Figure 1. Load-deformation curve demonstrating elastic and plastic regions of bone. Young's modulus (E) equals the slope. The vertical line represents stress applied, and the horizontal line represents strain. Adapted from Sharir et al., 2008.

Stress generates loads of axial compression, torsion and bending (RAHN, 2002). Strength can be defined as the ultimate load a material can withstand without breaking (ATHANASIOU et al., 2000). The type of loading and the rate it is applied determines the fracture configuration. Bone shows resistance to compression and usually fails by shear forces (ROE, 1998). Bone has an optimum mass-to-strength ratio due to the arrangement of its microstructures and also because of its inner cavities (BONUCCI, 2000). The material's stiffness is called shear modulus (MARTIN; BURR; SHARKEY, 2013). Bone stiffness is strain-rate dependent; that means that when load is applied there is an increase not only in the strain-rate but in the stiffness in a small amount (SHARIR; BARAK; SHAHAR, 2008). Bone's stiffness and strength are always

higher in the long axis, varying widely over the range of observed densities and depending on the rate and direction of loading (ATHANASIOU et al., 2000). Elastic modulus and strength are substantially lower in the transverse direction because the collagen and mineral crystals are lengthwise aligned (AUTEFAGE, 2000). Both femur and humerus suffer greater rotational forces if compared to tibia and radius due to larger cortical portion that results in greater polar moment of inertia (PMI) (MARKEL et al., 1994). PMI defines the dimension of a structure on a determined plane considering its ability to resist torsional loads (MARTIN; BURR; SHARKEY, 2013; ROE, 1998).

2.2 Mechanical Testing

Mechanics relates to the physical science that studies the effects of static (at rest) and dynamic (moving bodies) forces upon determined objects (AN et al., 2000). The standards static tests provide accurate and sensitive assessment of the biomechanical properties of bone and measure the forces applied to an object. Such forces can be axial (tensile and compressive), bending and torsion, static or cyclic (ATHANASIOU et al., 2000; GIBSON et al., 2008). Those are the forces that bones are subjected to during stance and ambulation and these tests closely simulate an *in vivo* loading condition (JEE, 2001).

Compression or tensile tests are very suitable to determine the behavior of osseous tissue under perpendicular loads. Specimens are compressed or tensioned and deform at various force coefficients – they exhibit lateral swelling or shrinking, depending on the vector's direction. Transverse strain values are proportional to the longitudinal ones (AUTEFAGE, 2000; MUIR; JOHNSON; MARKEL, 1995). When

loaded in compression a material becomes shorter in the stress direction but enlarged in the transverse orientation (MARKEL et al., 1994) as can be observed *in vivo* in vertebrae (AN et al., 2000). The proportion between transverse strain values and longitudinal strain components is characterized by Poisson's ratio (ν) (AUTEFAGE, 2000; SHARIR; BARAK; SHAHAR, 2008). Poisson's ratio is dimensionless and relates to the material's properties. Incompressible materials have around 0.5 ratio (like rubber) and the typical value for bone is 0.3 (MARKEL et al., 1994). Zero would be applicable to porous materials (AUTEFAGE, 2000). That means that the volume of matter tested cannot diminish or increase as a response to simple tensile and compressive load (AN et al., 2000).

Bending tests cause tensile force on one side of the bone and compressive stress on the other and can be performed on either three-point or four-point loading configuration (MUIR; JOHNSON; MARKEL, 1995; TURNER; BURR, 1993). Load applied and displacement at the point of failure are measured, creating thus a force-deflection graphic (SHARIR; BARAK; SHAHAR, 2008). Stress and strains are maximal at the surfaces receiving the load and zero at the neutral axis. Inertia, Newton's first law, determine that all matter remain at rest or in uniform motion in a determined direction unless an external force changes that state (AN, et al. 2000). Therefore, Area Moment of Inertia (AMI) is the fundamental characteristic that explains the ability of a material to resist bending and is inversely proportional to the stress applied of a section under bending forces (SHARIR; BARAK; SHAHAR, 2008). The major factors determining bending stiffness are area moment of inertia (AMI) and modulus of elasticity (MUIR; JOHNSON; MARKEL, 1995).

Torsion tests (twisting moment) measure bone's biomechanical peculiarities in

shear stress (ATHANASIOU et al., 2000). Torsion is naturally induced on normal weight bearing and can be very complex to assess (ROE, 1998). In order to perform this type of test, the bone's epiphyseal ends must be embedded in blocks of plastic material made to fit the grips of the testing machine. Torque is applied to one of these grips while the other epiphysis is kept steady, whilst load and angular deformation are recorded (SHARIR; BARAK; SHAHAR, 2008). Deformation stress varies from zero, at the center, to the maximum at the specimen's surface. The formula used to determine the value of shear stress (τ) is:

$$\tau = Tr/J$$

Where T is the torque applied, r is the maximum radial distance from the center to the surface of the cross section and J is the polar moment of inertia (PMI) (ATHANASIOU et al., 2000). Implant's PMI is not normally a weak point on the construct and rotational instability can be measured by fragments interaction (ROE, 1998).

2.3 Femoral fractures

Femur is a long bone, with medullary canal, that articulates with the hip and knee joints (MARKEL et al., 1994). Long bone fractures are usual in small animal practice and are commonly secondary to musculoskeletal injuries (LARIN et al., 2001). Femoral fractures account for approximately 20 to 25% of all occurrences reported in small animals (LARIN et al., 2001; WHITEHAIR; VASSEUR, 1992). The type of fracture has direct relation to the type of loads that produced it. It is expected that a higher energy

accumulation within the bone, when fracture occurs at a high strain rate, will likely result in more severe injury such as fracture comminution and extensive soft tissue damage (AUTEFAGE, 2000).

2.4 Fracture healing and Internal Fixation

Fracture healing depends on several factors, such as the natural stability of the fracture, effectiveness of reduction, implant's stiffness, patient's activity level and early weight bearing (STIFFLER, 2004). Internal fixation is recommended to aid bone healing and must consider biologic, mechanical and clinical aspects from each patient and fracture (ARON; JOHNSON; PALMER, 1995). Postoperative care and follow up are determinant for a successful outcome (LARIN et al., 2001; STIFFLER, 2004).

If perfect anatomical reconstruction is achieved, with absolute stable internal fixation, there will be direct (osteonal) healing with cortical remodeling without callus formation (AUGAT et al., 2003; PIERMATTEI; FLO; DECAMP, 2006). With less rigid fixation, where there is intermittent bone contact, there will be indirect bone healing characterized by callus formation and enchondral bone formation. Secondary or indirect healing is achieved in less precise biological repair with callus formation, unlike the anatomic reconstructed fractures (MARSELL; EINHORN, 2011). Bone is remodeled due to mechanical stresses on the called Wolff's law that defines that the loads applied to bones cause bone strains that generate signals detected by cells and to which they can respond and control modeling and remodeling (FROST, 2004).

The amount of motion and interaction between bone fragments, stress variation and deformation across the callus define the mechanical environment, with direct

influence on cell differentiation and tissue formation on the fracture-healing biology (ROE, 1998). Interfragmentary motion consists on the sum of the spatial displacements on the proximal segment, compared to the distal margin of the gap (BERNARDE et al., 2002). It is generally accepted that high rates of movement on the fracture site obstruct the invasion of blood vessels and the differentiation of pluripotential tissue into bone. That can be followed by bone resorption and possible delayed union or even nonunion cases because the level of motion among the fragments influence fracture healing patterns (DAILEY et al., 2012). As deposition of cartilage matrix occurs, even lower cellular resistance to deformation is allowed, otherwise cartilaginous and fibrous tissue differentiation may occur (AUGAT et al., 2003).

It is known that controlled axial interfragmentary micromotion can be anabolic to callus formation and new bone deposition. It stimulates osteoblastic activity including proliferation and synthesis and both excesses stability and instability must be avoided to prevent their detrimental effect (DAILEY et al., 2013). Therefore, the internal fixation apparatus must be rigid enough to prevent excessive interfragmentary strain but must also be flexible enough to share load with the bone while fracture repair occurs (GAUTHIER et al., 2011). Ovine models showed that interfragmentary shear can delay healing compared to axial or movement of an equal proportion (AUGAT et al., 2003).

It has been suggested that optimal axial interfragmentary movement seems to be within the range 0.2 – 1 mm to animals and is important during remodeling phase of the callus (DUDA et al., 1997). A study was conducted by Yamaji et al. (2001) to identify the suitable amount of micromovement on sheep's metatarsi fracture sites stabilized with external ring fixation that allowed defined axial micromovements. There were four groups of animals, with gaps of 2 mm and 6 mm and micromovements of 0.3

mm and 0.7 mm respectively. In the fourth week of experiment, large micromovements in a small gap resulted in increased bone formation, whereas, for large gaps, the large micromovements diminished new bone formation.

Many different fixation methods can be applied for aiding femoral fractures including pins, cerclage wire, screws, different types of plates, external skeletal fixators and interlocking nails or even a combination of those techniques (LARIN et al., 2001; STIFFLER, 2004). It has been introduced recently the use of clamp rod internal fixation (CRIF) for small animals (BONIN et al., 2014). Each of these methods transmit specific levels of stability to a fracture and must be chosen carefully (STIFFLER, 2004).

In the past the premise for fracture treatment was open reduction and internal fixation (ORIF) with perfect anatomic reconstruction and rigid stabilization as AO/ASIF (Arbeitsgemeinschaft für Osteosynthesefragen / Association for the Study of Internal Fixation) recommended, which could lead to iatrogenic surgical trauma for the surrounding soft tissues (DÉJARDIN; GUIOT; VON PFEIL, 2012; STIFFLER, 2004). AO concepts were first introduced to veterinary medicine in the mid-1960s and established guidelines for functional recovery to encourage early weight bearing after orthopedic intervention with techniques of anatomical fragment reduction, atraumatic surgery and the use of rigid fixation to foster rapid restoration of the affected limb's function (SCHATZKER, 2005). Nonetheless, this method of fracture repair would be accompanied by complications such as delayed or even nonunion, infection and also implant failure (DÉJARDIN; GUIOT; VON PFEIL, 2012).

Recent review of clinical outcomes of the AO method led to a philosophy shift toward focusing on biological priorities as avoidance of soft tissues damage and preservation of the extraosseous blood supply during fracture stabilization. Perfect

anatomic reconstruction was deemphasized unless it involves intra-articular fractures, those require perfectly congruent surface to avoid post-traumatic arthritis (HORSTMAN et al., 2004; PERREN, 2002). The proposition of biological osteosynthesis is to align the main fracture segments with minimal surgical exposure in closed fashion through the use of fluoroscopy and to insert the implants through minimal incisions or if necessary with an "open-but-do-not-touch" (OBDNT) technique (HUDSON; POZZI; LEWIS, 2009; JOHNSON, 2003). The essential feature of the OBDNT technique consists on the smallest possible incisions with low exposure of the main fragments and minimal disturbance of periosteal soft tissues in order to preserve the fracture hematoma (HORSTMAN et al., 2004; PALMER, 1999). This is called minimally invasive osteosynthesis (MIO) and has the purpose of using a fixation method able to maintain proper alignment and bone length while repair occurs without ever exposing the fracture site (DÉJARDIN; GUIOT; VON PFEIL, 2012; PERREN, 2002; STIFFLER, 2004). MIO has reduced surgical time, decreased blood loss and diminished risk of postoperative infection (DÉJARDIN; GUIOT; VON PFEIL, 2012; HORSTMAN et al., 2004; PALMER, 1999). Interfragmentary screws, cerclage wires and the disruption of fracture are not the main choices with MIO. Rather plates or interlocking nails are preferred to provide stabilization through indirect reduction and small approaches to the bone (DÉJARDIN; GUIOT; VON PFEIL, 2012).

As the fracture hematoma suffers minimum manipulation, osteoinductive properties are preserved within the undisturbed biologic environment (DÉJARDIN; GUIOT; VON PFEIL, 2012; HUDSON; POZZI; LEWIS, 2009; PERREN, 2002). Attention is given to reestablishment of bone alignment and obtaining proper construct stability instead of focusing on perfect anatomical reduction and rigid interfragmentary

compression (DÉJARDIN; GUIOT; VON PFEIL, 2012).

2.5 Interlocking Nails

Interlocking nails (INs) are solid intramedullary nails with transverse openings (holes) at both extremities or sometimes along the length of the construct for screw or bolt insertion, to anchor the nail on the bone (DÉJARDIN et al., 2006; DÍAZ-BERTRANA et al., 2005; ENDO et al., 1998). Usually the screws or bolts lock the nail in the bone by engaging the cis- and trans-cortices creating the nail/bone construct. Their proximal extremity engages rigidly with an alignment guide via extension rods while the distal end consists of a dull or trocar point on the commercially available models (DÉJARDIN; GUIOT; VON PFEIL, 2012). Veterinary INs are normally made of stainless steel (STIFFLER, 2004) but a custom-made titanium IN has been reported (SCOTTI et al., 2007).

INs are available in several diameters and lengths in veterinary medicine. The usual diameters range from 4 to 10 mm with variable lengths and a small novel customized IN for cats with 3.5 mm has been described (SCOTTI et al., 2007). The holes of INs must be kept at a minimum distance of 2 cm from the fracture line (DUELAND; VANDERBY; MCCABE, 1997) and the distance between holes varies between models. Screws or bolts come on different sizes to suit the nail diameter. The locked construct can resist torsional, compressive, and shear forces (DÉJARDIN; GUIOT; VON PFEIL, 2012).

The idea of treating long bone fractures with intramedullary nailing emerged from the nail with a longitudinal slot on its length proposed by Küntscher in the early 1940s (DUELAND; VANDERBY; MCCABE, 1997; KÜNTSCHER, 1958) and evolved

with the development in 1975 of a IN to treat femoral fractures in people (HUCKSTEP, 1975). Modified Huckstep nails were introduced into veterinary medicine in the 1980s and 1990s with success (DURALL; DIAZ; MORALES, 1993; JOHNSON; HUCKSTEP, 1986; MUIR; JOHNSON, 1996). They were followed by the development of a variety of specially designed nails for veterinary medicine in different countries (ARON; JOHNSON; PALMER, 1995; DÉJARDIN et al., 2006; DUELAND et al., 1996; DURALL; DIAZ; MORALES, 1994; ENDO et al., 1998). The two most used systems in the United States are the standard nail system called The Original Interlocking Nail System™ from Innovative Animal Products and the I-Loc® that features an hourglass profile (DÉJARDIN; GUIOT; VON PFEIL, 2012).

INs are used in small animal surgery for fractures involving usually the femur, humerus and tibia (DÉJARDIN; GUIOT; VON PFEIL, 2012; LARIN et al., 2001) but the use on proximal radio-ulnar fracture on a dog has been described (GATINEAU; PLANTÉ, 2010). The size of the nails can significantly limit their use in small patients in which the implant might be too big for the restricted intramedullary canal's size (DÍAZ-BERTRANA et al., 2005; LARIN et al., 2001). Most interlocking nails systems currently in use also require complex instrumentation and aiming guides for their application and to allow screw holes to be drilled accurately (DÉJARDIN; GUIOT; VON PFEIL, 2012).

Minimally invasive nail osteosynthesis (MINO) techniques have clinical advantages over anatomical reconstruction: noted reduction in surgical time and healing interval without enhance of complication rates. These techniques preserve periosteal blood supply, require less surgical exposure and dissection due to limited approaches when compared to bone plates, have lower infection rates, decreased

incidence of bone healing problems and diminished hospitalization period (DÉJARDIN; GUIOT; VON PFEIL, 2012; HORSTMAN et al., 2004; REEMS; PLUHAR; WHEELER, 2006).

IN's characteristics such as diameter, material properties, wall thickness, curvature and cross-sectional shape are determinant for their mechanical properties (KINAST; FRIGG; PERREN, 1990). INs are placed near the neutral axis of the bone and therefore are shielded against cyclic bending (DÉJARDIN; GUIOT; VON PFEIL, 2012). They usually don't share load with the fragments allowing indirect bone healing and callus formation with biomechanical reinforcement (LARIN et al., 2001; STIFFLER, 2004) not by creating elastic jamming in the medullary cavity but by the connection between the nail and the bolt (SCHANDELMAIER et al., 2000). Mechanical advantages of INs in bending and shear are similar to those of large intramedullary rods but with the added benefit of resisting torsion and compression due to their locking mechanisms. When compared to bone plates used for similar fractures, INs have a larger area moment of inertia; resulting in a much improved bending stiffness (MUIR; JOHNSON; MARKEL, 1995; SCHANDELMAIER et al., 2000). Biomechanical comparison of INs and plate-rod constructs described exceptional resistance to bending and flexion by INs, however rotational instability (slack) was observed (VON PFEIL et al., 2005). An hourglass-shaped IN designed by Déjardin et al. (2006) showed no slack under torsional forces and the authors concluded it to have better torsional stability than the INs available at that time. Further *in vivo* studies, clinical findings and *ex vivo* biomechanical comparison suggest that this new device provides a postoperative biomechanical environment more conducive to bone healing than a comparable standard IN (DÉJARDIN et al., 2014).

Torsional instability on IN is a result of the discrepancy between the nail hole diameter and the diameter of the bolt and this effect may be exacerbated under torsion (VON PFEIL et al., 2005). Some authors have described the use of adjuvant techniques to enhance INs stability (BASINGER; SUBER, 2004; NANAI; BASINGER, 2005) but the benefits of such practice can be doubted since they can debilitate the biological concepts for fracture repair (DÉJARDIN et al., 2006). It is recognized that excessive torsional and shear motions have undesired effects such as prolonging bone healing and function recovery periods (AUGAT et al., 2003; KLEIN et al., 2003), but the correct amount of shear forces is desirable and can cause augmentation in callus formation (PARK et al., 1998). INs are weaker in mediolateral bending because the AMI of the nail is smaller in a bending plane that is parallel to the screw hole (MUIR; JOHNSON; MARKEL, 1995).

The main complication reported is breakage or bending of the nail (DUHAUTOIS, 2003; HORSTMAN et al., 2004). According to Dueland et al. (1999), breakage is due to material fatigue and by use of nails with insufficient diameter and improper positioning. Other reported aggravations are loosening of bone implants, delayed or non-union, damage to locking screws, infection, nerve injury in the area of locking screw fixation, muscle contracture and pseudarthrosis (DÉJARDIN; GUIOT; VON PFEIL, 2012; DÍAZ-BERTRANA et al., 2005; DUHAUTOIS, 2003; DURALL; DIAZ, 1996; LARIN et al., 2001). Reaming, a practice that allows for the implantation of larger nails and locking devices, used to be recommended by some authors but can severely impair the intramedullary blood supply and is associated with higher infection rates and also to fat embolism, therefore fell into disuse (KLEIN et al., 2003). In a retrospective study of 121 cases of long bones fracture in dogs and cats, repaired with

veterinary INs in 2003, 8% of patients required a second surgery to achieve bone healing (related to the degree of comminution). There were failures because of error selecting nail diameter or length (n=3) and nonunions due to locking error (n=2). Overall 93% of the patients healed with excellent functional outcome (DUHAUTOIS, 2003).

Studies have demonstrated that stress is markedly high at the distal screw of an IN, place of frequent mechanical failure. The extension of contact between the nail and cortical bone, the distance from the distal locking screw and the fracture site, the number of screws on the jig and the length of the locking screw can affect this type of stress (LIN et al., 2001). The weakest point on an IN is the screw hole and that is not diminished by the placement of a screw on such hole (ROE, 1998). The holes act as stress concentrators and may result in fatigue failure of the screw or bolt (DÉJARDIN et al., 2006; REEMS; PLUHAR; WHEELER, 2006). The size of nail hole and locking bolt directly affect the strength and failure patterns of INs (AUGAT et al., 2003; GAEBLER et al., 2001; LIN et al., 2001). On comminuted fractures the IN acts as a load-bearing construct initially (APER et al., 2003), until the healing starts with greater mechanical stability to share the load with the bone (EVELEIGH, 1995).

On a study conducted by Dueland et al. (1999), breakage of the IN through a screw hole was reported in 14% of cases. INs show weakness at the screws holes because the locking screws or bolts do not interact rigidly with the nail and therefore do not help to reduce the stresses as they would on a locking compression plate (APER et al., 2003). Dynamic compression plates (DCP) can also undergo excessive cyclic bending on empty screw holes when perfect anatomical reconstruction is not achieved due to its eccentric placement or when there is no transcortical support, which leads to

implant failure specially in cases of delayed bone union (VON PFEIL et al., 2005).

Screw failure depends on its bending stiffness. Small decreases on its core diameter result in substantial decreases on the bending stiffness (MUIR; JOHNSON; MARKEL, 1995), therefore screws with larger core diameter are more resistant (LIN et al., 2001). Bolts usually have a larger core diameter than screws, therefore are stronger and stiffer than screws (BURNS et al., 2011; STIFFLER, 2004). Under axial strain, screws and bolts are subjected to 4-point bending forces and their mode of failure usually relates to bolt bending or breaking (REEMS; PLUHAR; WHEELER, 2006). Aper et al. (2003) tested the effects of eccentric loading on the fatigue life of cortical bone screws on INs and concluded that eccentric loading of the locking screw in the metaphyseal region may improve its fatigue life, which happens naturally on the curvilinear nature of canine bone. On similar study with bolts, Burns et al. (2011) concluded that placement of the bolt in metaphyseal bone extends its fatigue life under axial loading and decreases the incidence of catastrophic failure under torsional loading.

In human orthopedics, new intramedullary devices were developed to treat specific fractures. There is the Targon® PH intramedullary nail to treat proximal humeral fractures (GRADL et al., 2007) and also a titanium elastic nail for clavicular midshaft fractures (FRIGG et al., 2009). There is the Angular Stable Locking System (ASLS) for distal tibial fractures (with significantly higher axial and torsional stiffness than regular INs) (KUHN, et al. 2014a), retrograde tibial nailing systems for distal tibia fractures (KUHN, et al. 2014b), elastic stable intramedullary nailing for pediatric fractures (BERGER et al., 2014), Flexible Axial Stimulation (FAST) IN (DAILEY et al., 2013). INs for fractures of the radius and ulna (SAKA et al., 2014) were also developed,

as well as INs for upper ankle joint fractures (malleolar fractures) (GEHR et al., 2004) and calcaneal intramedullary nails (GOLDZAK et al., 2014).

2.6 Targon® Vet Nail System

A new device – the Targon® Vet Nail System (TVS) (Aesculap B. Braun Vet Care, Tuttlingen, Germany) has been recently adapted from human trauma and introduced for veterinary use. It works differently than the currently available IN systems: it consists of a smaller intramedullary rod that do not require reaming of the medullary cavity, inserted and locked in a hole that goes through large locking bolts that can be positioned at the discretion of the surgeon to fit the individual patient (Figure 2A). This locking mechanism differs significantly from those of conventional nails and consists of the bolt gripping the intramedullary nail, as opposed to the screw fitting inside a hole in the nail itself. This method may decrease the amount of torsional slack observed in some traditional nails (DÉJARDIN et al., 2006) but may be more prone to slippage. The system requires its own amount of specialized instruments and no aiming device or fluoroscopy are essential for placement. Adjustments on length and rotation are possible after insertion (BRÜCKNER; UNGER; SPIES, 2014).

The locking bolts of the TVS consist of two parts (Figures 2B and 2C). One part is anchored in the trans-cortex and has a self-tapping thread and another thicker part, hollow to engage the fixing screw, placed in the medullary cavity and cis-cortex. The holes for bolts' implantation are drilled with specially designed drill guides. A 4.8 mm hole is drilled into the cis-cortex and a 2.8 mm hole into the trans-cortex. Only the cis-cortex hole is tapped and the locking bolt is inserted with a special screwdriver that

has a clamping nut that holds the bolt in the correct position so that the oblong hole inside the bolt is aligned for the insertion of the intramedullary nail (BRÜCKNER; UNGER; SPIES, 2014). The system comes in two sizes: 3 mm and 2.5 mm, the smallest available.

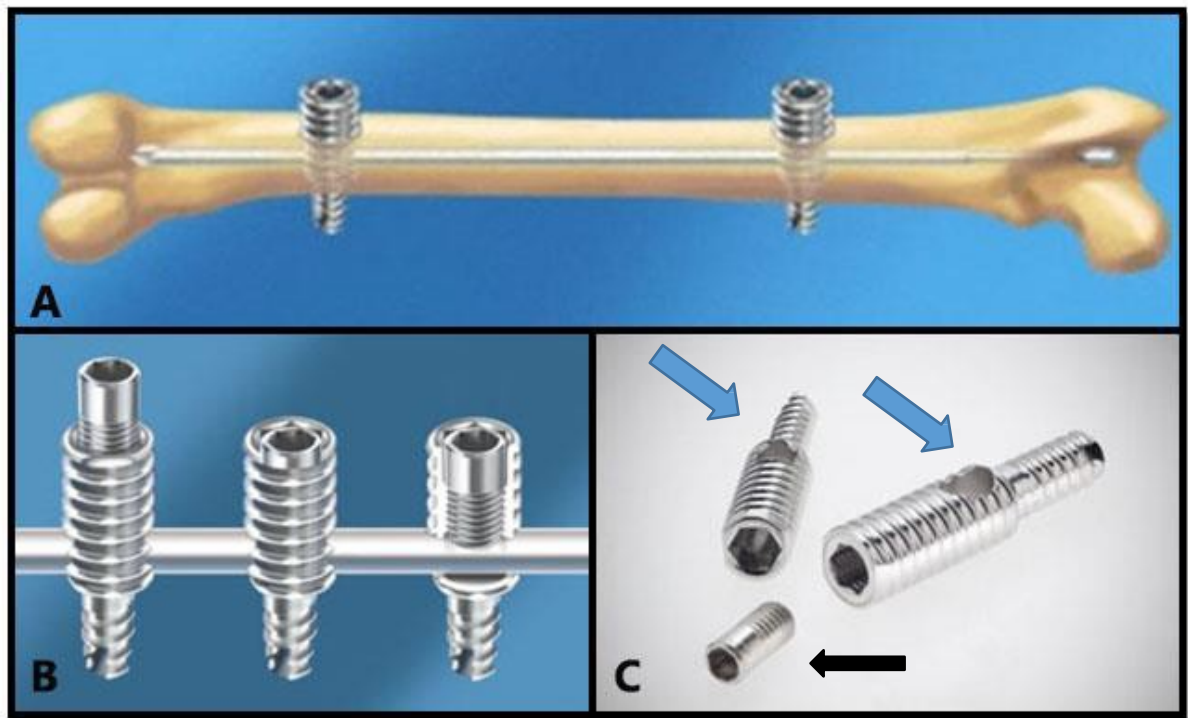


Figure 2. Targon® Vet Nail System (TVS). A) Schematic drawing of the TVS applied to a feline femur. B) Schematic drawing of the locking mechanism. The fixing screw fits inside the bolt and locks the construct with the nail. C) Picture of two locking bolts (blue arrows) and one fixing screw (black arrow). Source: B. Braun Vet Care GmbH, 2015.

Preliminary studies of the Targon® Vet Nail System were performed on saw bone models and laminated/gripped paper tubes to evaluate biomechanical properties (Aesculap-unpublished data). Non-destructive compression test was performed and because the femurs were placed in a standardized weight bearing position for testing, the natural anteversion of the femoral neck provided a small amount of torsion during testing (0.69 Nm). In this experiment, no difference was observed between the nail and

a 2 mm plate. More stringent torsional testing was performed to evaluate the torsional resistance of the bolts' gripping system on the rod. Although tested to failure, they were performed on cardboard surrogate and therefore the results cannot be extrapolated to bones. In another study, the influence of the bolt's hole size was tested to see its effect on feline femurs and the stability of the construct was compared to a DCP on a femoral fracture gap model. The authors concluded the stability of the construct is at least comparable to a DCP plate with more micromotion allowed due to the smaller size of the pin in the medullary canal and that the minimal diaphyseal bone diameter safe for bolt insertion is 8.5 mm, a limiting factor to the TVS applicability (BRÜCKNER; UNGER; SPIES, 2014). It has been shown previously that holes drilled into cortical bone significantly weaken the bone, particularly in torsion and they should not exceed 20-25% of the bone diameter for risk of iatrogenic failure (GIBSON et al., 2008; JEE, 2001).

Furthermore, slack of slippage under cyclic loading was not evaluated. The risk of bone failure through the holes in the bone was assessed in bending but not in torsion. As bone is more prone to fail in torsion than bending, the results likely overestimate the strength of the constructs. Bone is a heterogenous material with different biomechanical properties along its length (JEE, 2001). It is reasonable to believe that the effects of the bolts placed in the metaphysis would be different from those obtained with the bolts placed into the diaphysis. A previous study using more traditional locking nail system has shown that the location of locking bolts did significantly influence the torsional strength and stiffness of nail constructs. On one hand, the shorter "working length" of the nail when bolts are placed closer to the fracture should increase stiffness of the system but, on the other hand, would likely

increase risk of failure and decrease its ultimate strength. Similar findings were observed for the Innovative™ nail (BURNS et al., 2011). Because of the relatively larger size of the bolts in the Targon® Vet System, this effect could be dramatically increased.

3. PURPOSE

The purpose of this study was to evaluate the torsional stability of the Targon® Vet Nail System in small canine femurs and to study the effect of different bolt locations on the torsional strength of the constructs compared to 2.4 mm LC-DCP® plates.

3.1 Specific Goals

To test the torsional strength and stiffness of the Targon® Vet Nail System during non-destructive cyclic testing in small canine femurs;

To test the effect of varying bolt location on the strength and stiffness of the construct during non-destructive cyclic testing;

To test the torsional strength and stiffness of LC-DCP® plates and compare it to the TVS.

3.2 Hypotheses

The location of the bolts will significantly influence the torsional properties of the Targon® Vet Nail System during non-destructive testing;

Slack will not be observed during non-destructive testing;

The location of the bolts will significantly influence the ultimate strength of the constructs in torsion.

The torsional strength of the TVS constructs will correspond to that from the LC-DCP® plates.

4. MATERIAL AND METHODS

Biomechanical torsional studies of the 2.5 mm Targon® Vet Nail System were performed to compare two different bolt locations on canine femur and to contrast with 2.4 mm LC- DCP® plates.

4.1 Ethic Considerations

The study was approved by the São Paulo State University Committee for Animal Use and Care (CEUA) under the protocol nº 009278/14.

4.2 Specimen collection

Thirty-six femurs were harvested from 18 dogs obtained from the local humane society. The dogs were euthanatized due to non-orthopaedic conditions and were stored at the Research Laboratory of the Ontario Veterinary College, University of Guelph, CA. The dogs were from both genders, all similar in size. Data was collected from the femurs to verify the inclusion criteria and compatibility with implant size. Through digital radiographic examination in orthogonal views, it was possible to screen the femurs for pre-existing trauma or bone abnormalities and measure the bones (Figure 3A). Specimens with radiographic abnormalities or without the criteria specifications were excluded from further analysis. A radiographic calibration marker was positioned adjacent to each femur and equidistant from the radiographic detector to achieve digital calibration and measurement of each femur. The images were

evaluated with commercially available templating software¹ for orthopaedic planning.

Inclusion criteria were femoral length (measured on craniocaudal view from the articular surface of the lateral condyle to the most proximal part of the greater trochanter) between 98 and 124 mm and the diaphyseal diameter (measured on craniocaudal view in the midpoint of the length line measured) higher than 8.5 mm (compatible with 2.5 mm Targon® Vet implants).

Bones were detached from their articular insertions and all soft tissues were removed with surgical instruments (Figure 3B), then specimens were identified and wrapped in towels soaked with isotonic saline (0.9% NaCl) solution, double sealed in plastic specimen bags, and stored at -20°C until testing.

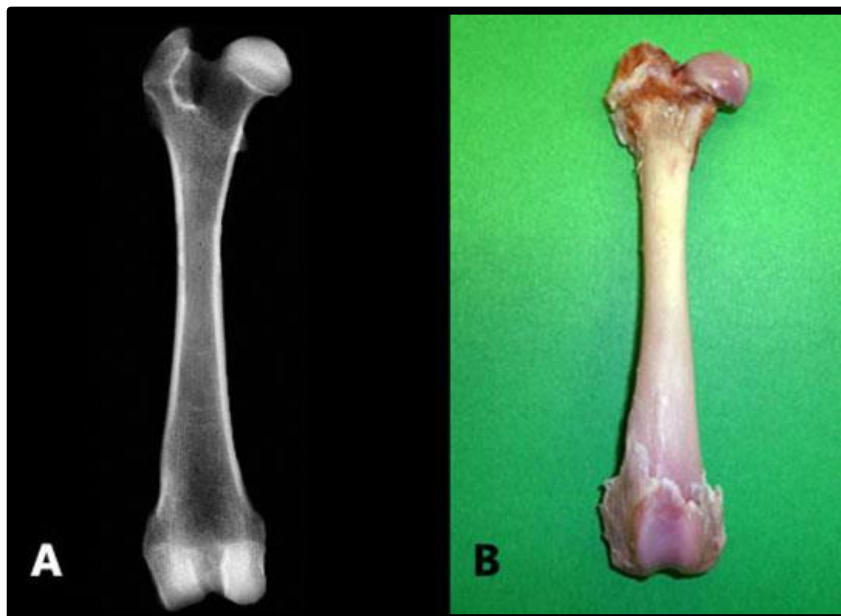


Figure 3. A) Craniocaudal (cr-ca) radiographic view of a right canine femur. B) Canine right femur after softer tissues removal. Guelph, 2014.

¹ Orthoview® - LLC, Jacksonville, Florida, US.

4.3 Implants

4.3.1 Targon® Vet Nail

Twenty-four units of 2.5 mm Targon® Vet Nail System² (TVS) (Figure 4A) with lengths adjusted to bone lengths were used in Groups 1 and 2 (n=24) with 48 locking screws with lengths between 16 and 22 mm (implant steel, material number 1.4441 X2CrNiMo18–15–3,316 LVM). The locking screw (Figure 4B) consists of two parts. One part that anchors in the trans-cortex, with self-tapping thread of 2.8 mm outer diameter, 2.2 mm of core diameter, and 1.2 mm of thread pitch. The second part is thicker to be placed in the medullary cavity and in the cis-cortex. It has 4.8 mm of outer thread with a thread pitch of 1.2 mm and is hollow to engage the fixing screw. Forty-eight fixing screws (Phynox alloying) with an outer diameter of 3 mm, a core diameter of 2.38 mm, and a thread pitch of 0.5 mm were used (Figure 4C), they were locked with 1.8 Nm of torque. The TVS were implanted on bones with the recommended surgical instruments (Figure 5).

² Aesculap B. Braun Vet Care, Tuttlingen, DE.

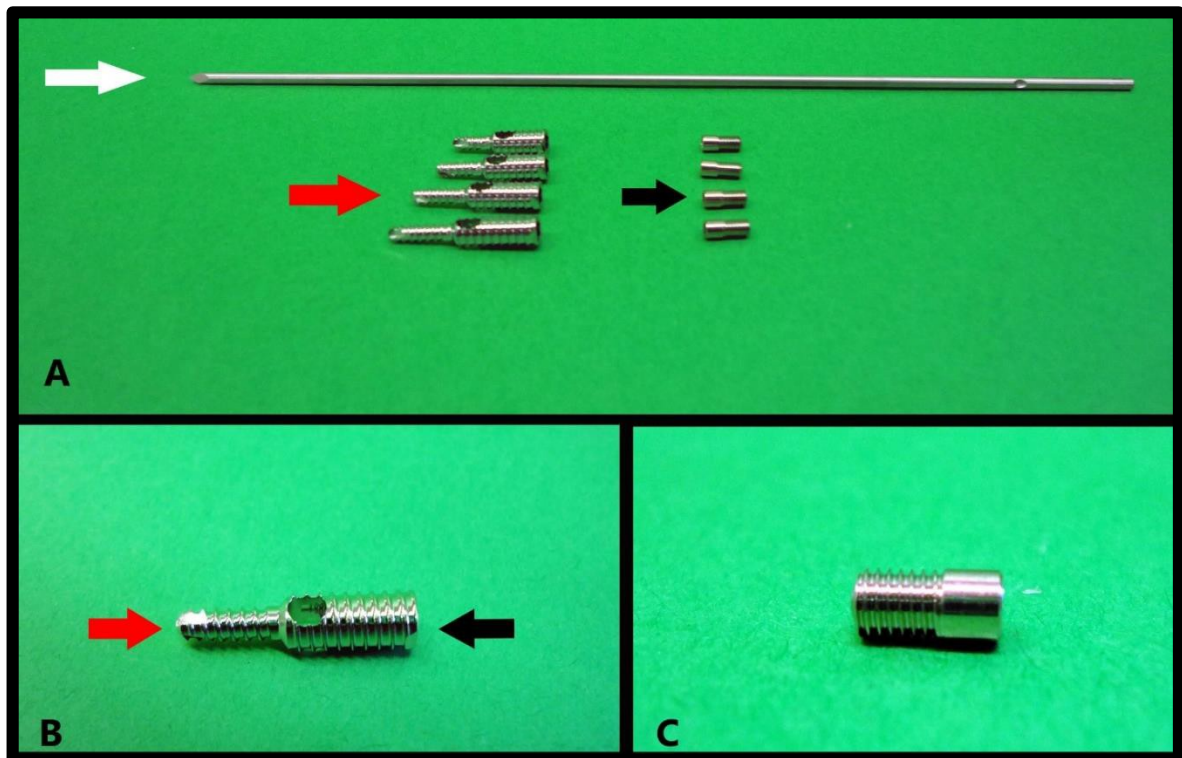


Figure 4. A) Targon® Vet Nail System (TVS) implants. Intramedullary nail with 2.5 mm of diameter (white arrow). Locking screws (red arrow) with lengths between 16 and 22 mm and fixing screws (black arrow) used to lock the TVS construct. B) Locking screw with on part of 2.8 mm of outer diameter (red arrow) and the thicker part with outer diameter of 4.8 mm (black arrow). C) Fixing screw with 3 mm of outer diameter. Guelph, 2014.

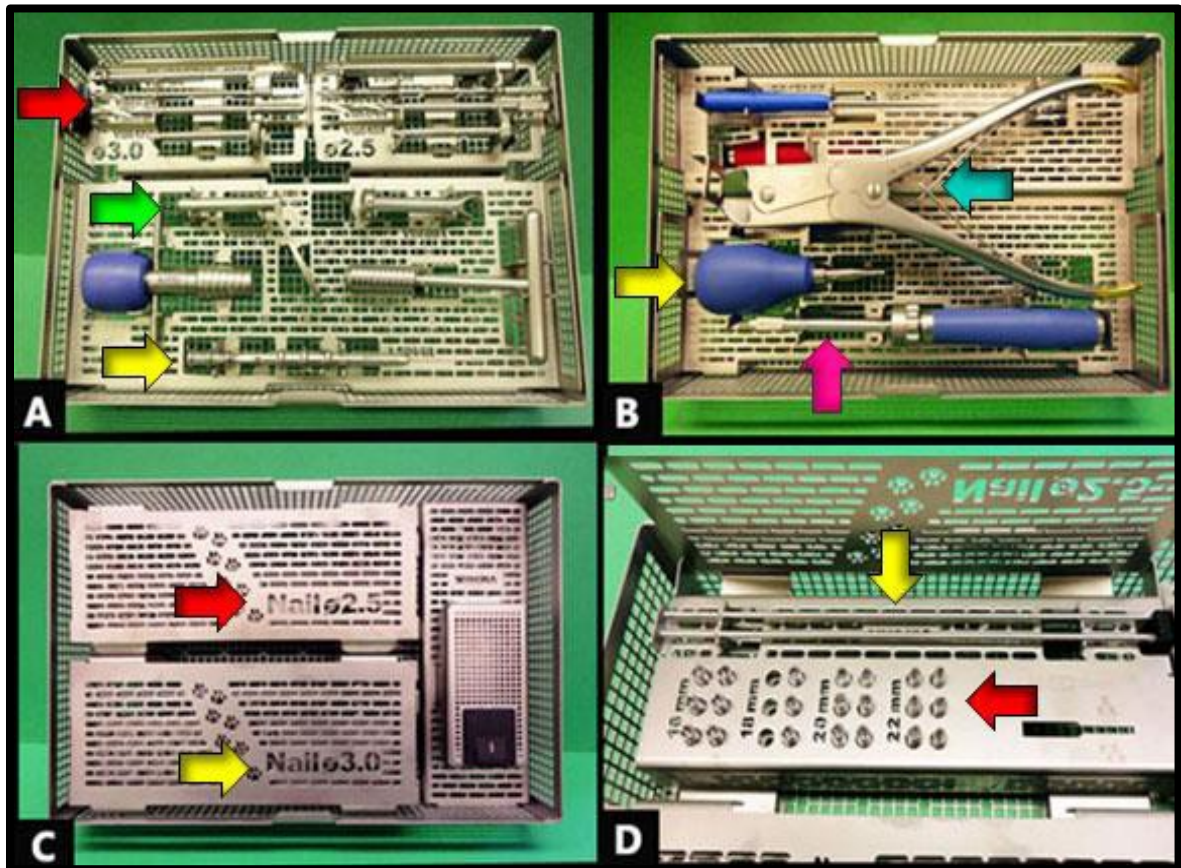


Figure 5. A) TVS instrument set box one: drill bits (red arrow), drill guides (green arrow) and depth gauge (yellow arrow). B) TVS instrument set two, with pin cutter (light blue arrow), torquimeter (yellow arrow) and screwdriver (pink arrow). C) TVS implants box with 2.5 mm (red arrow) and 3 mm implants (yellow arrow). D) 2.5 mm implants on detail with nails (yellow arrow) and screws (red arrow). Guelph, 2014.

4.3.2 -DCP® Plates

Twelve units of 7-hole 2.4 mm limited contact, dynamic compression plates³ (LC-DCP®) made of 316 L steel (Figure 6A) were used in Group 3 (n=12), with 72 units

³ Synthes Canada, Mississauga, CA.

of 2.4 mm cortical self-tapping screws⁴ of lengths between 18 and 22 mm (Figure 6B).

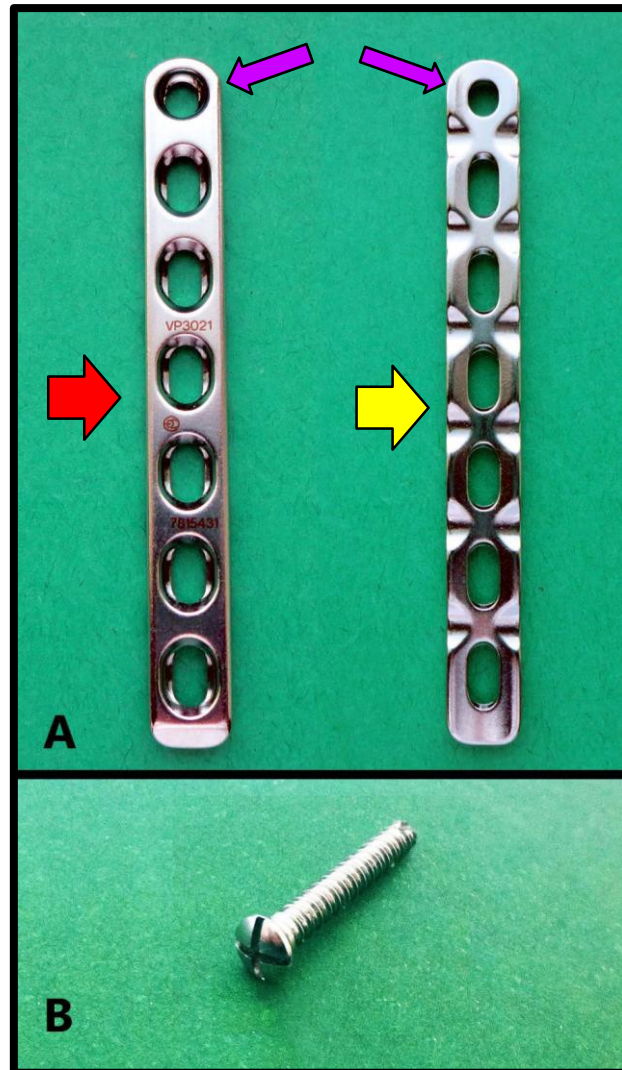


Figure 6. A) Picture of two 7-hole 2.4 mm limited contact, dynamic compression plates (LC-DCP®). Note the superior part of the plate where the screws are inserted (red arrow), and the inferior part that faces the bone (yellow arrow). The first hole of the plates are rounded for screw insertion in neutral position (purple arrows), while the others are elliptical to fit both neutral screws or in compression mode. B) Picture of a 2.4 mm self-tapping cortical screw. Guelph, 2014.

⁴ Synthes Canada, Mississauga, CA.

4.4 Specimen preparation

Twenty-four hours prior to testing, the femurs were thawed at room temperature. Moisture of all specimens was maintained by use of isotonic saline solution during all preparation and testing procedures.

Group 1: Femurs were prepared with TVS construct in accordance with the manufacturer's recommendations with special surgical equipment. In all bones, points immediately below the lesser trochanter and just above the fabellae were marked (Figure 7A). The distance between these two points was measured and defined as "X" (Figure 7B). A line was crossed in the mid distance between the two marks and the screw holes were drilled with a 4 mm drill in the cis-cortex through use of a specially designed drill guide (Figure 8A to 8D). The next step was to insert an special drill guide for the trans-cortex in the hole and use the 2 mm drill in the trans-cortex (Figures 9A to 9C).

After both holes were drilled (Figure 10A), their depths were measured with a depth gauge and the cis-cortex was tapped (Figure 10B). The locking bolts were inserted in a lateral to medial direction, the proximal bolt was located right underneath the lesser trochanter and the position of the distal bolt was just above the femoral condyles, as it would be done in a clinical case of diaphyseal fracture. A transverse osteotomy was performed equidistant to the bolts. Reaming of the femoral medullary cavity was not necessary. A 2.5 mm intramedullary nail was inserted (Figure 11A) and locked with the fixing screws with 1.4 Nm torque with use of a special torque wrench (Figure 11B).

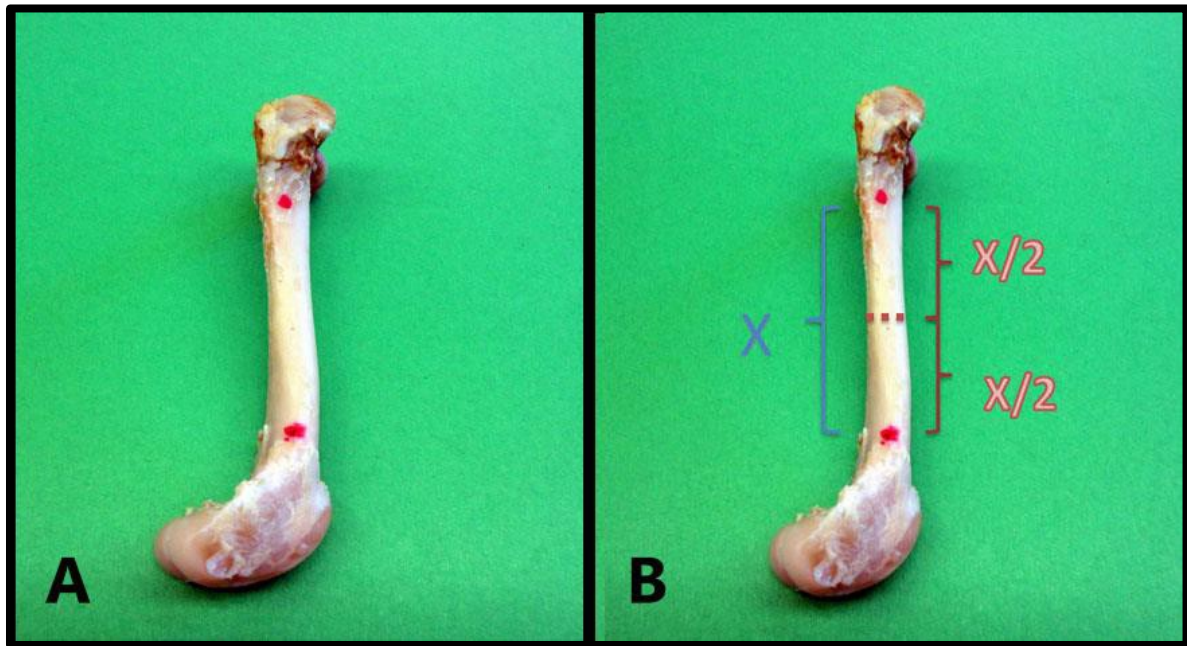


Figure 7. A) Canine right femur with the points immediately below the lesser trochanter and just above the fabellae marked (red dots). B) After the points were marked, the distance between them was measured (X), and the midpoint was defined as the osteotomy line. Guelph, 2014.

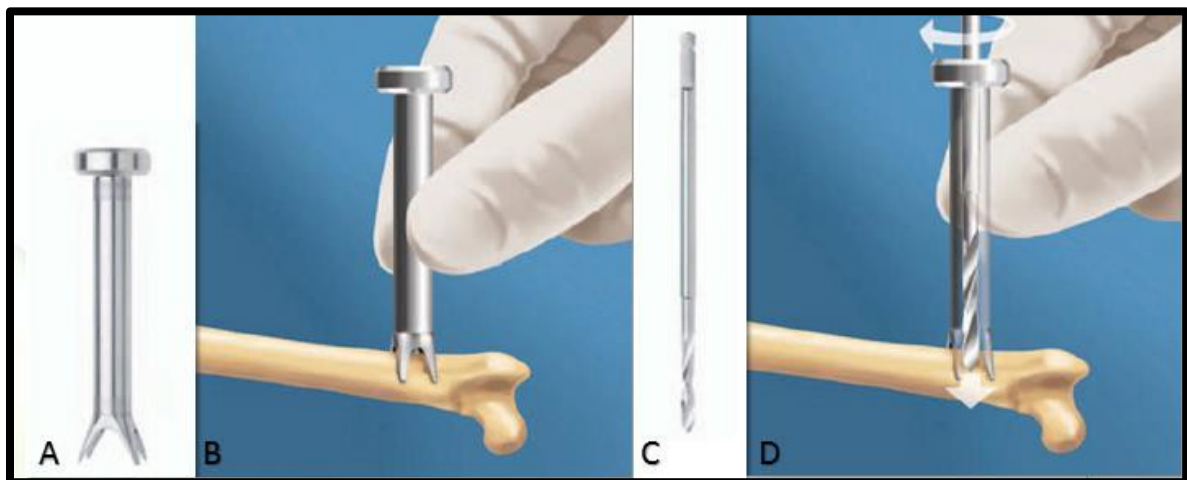


Figure 8. A) Picture of centering drill sleeve. B) Drawing of positioning the drill sleeve to drill the cis-cortex hole. C) Picture of the 4 mm drill bit. D) Drawing of the drilling procedure of the cis-cortex. Source: B. Braun Vet Care GmbH, 2015.

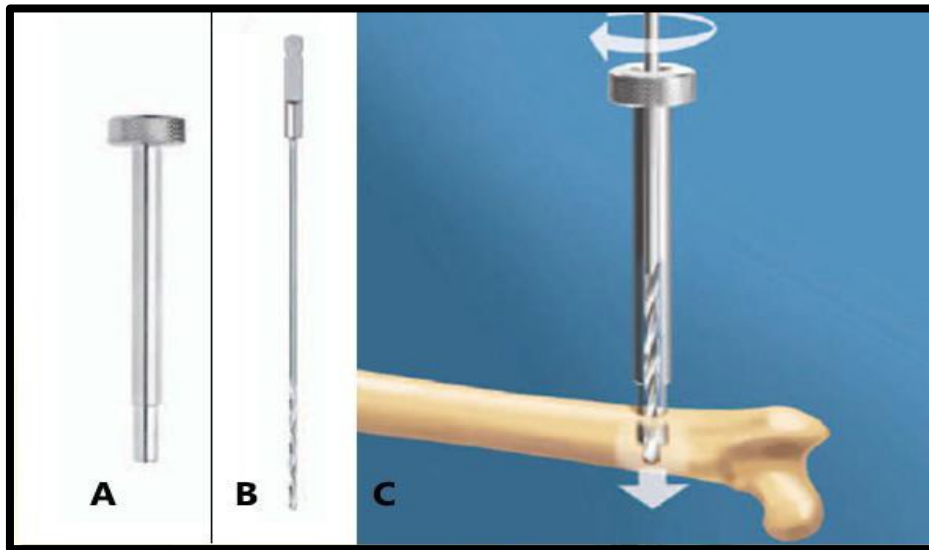


Figure 9. A) Picture of drill sleeve with internal diameter of 2.5 mm that fits the cis-cortex hole. B) Picture of a 2.5 mm drill bit. C) Drawing of the sleeve being inserted through the cis-cortex hole and drilling of the trans-cortex by the 2.5 mm drill bit. Source: B. Braun Vet Care GmbH, 2015.

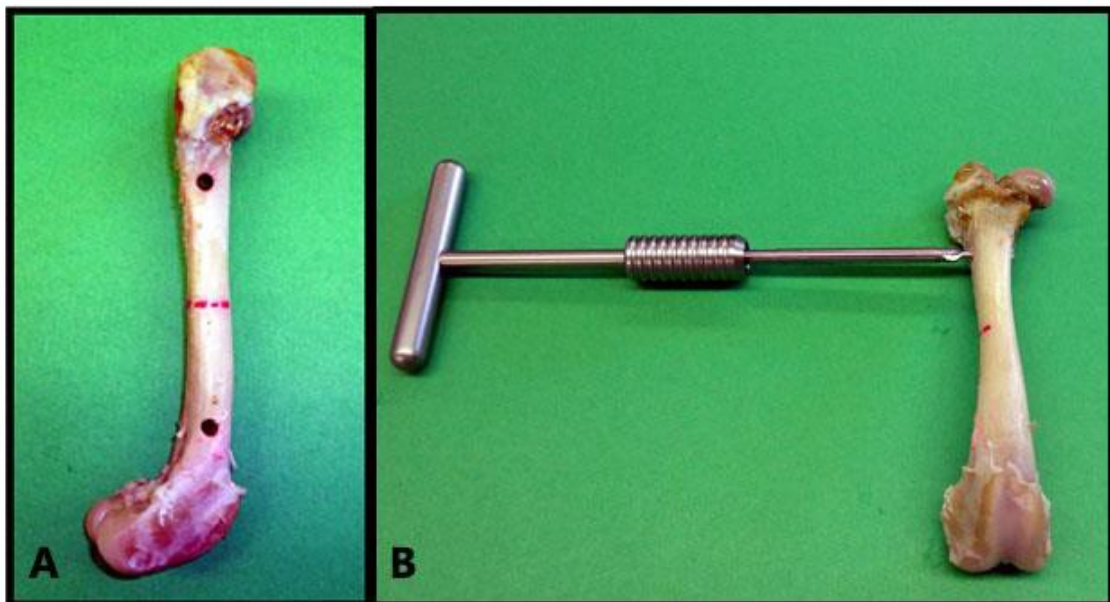


Figure 10. A) Picture of a canine right femur from Group 1. Note the osteotomy line crossed in the mid distance between the two holes drilled. B) Picture of the same femur having the cis-cortex tapped. Guelph, 2014.

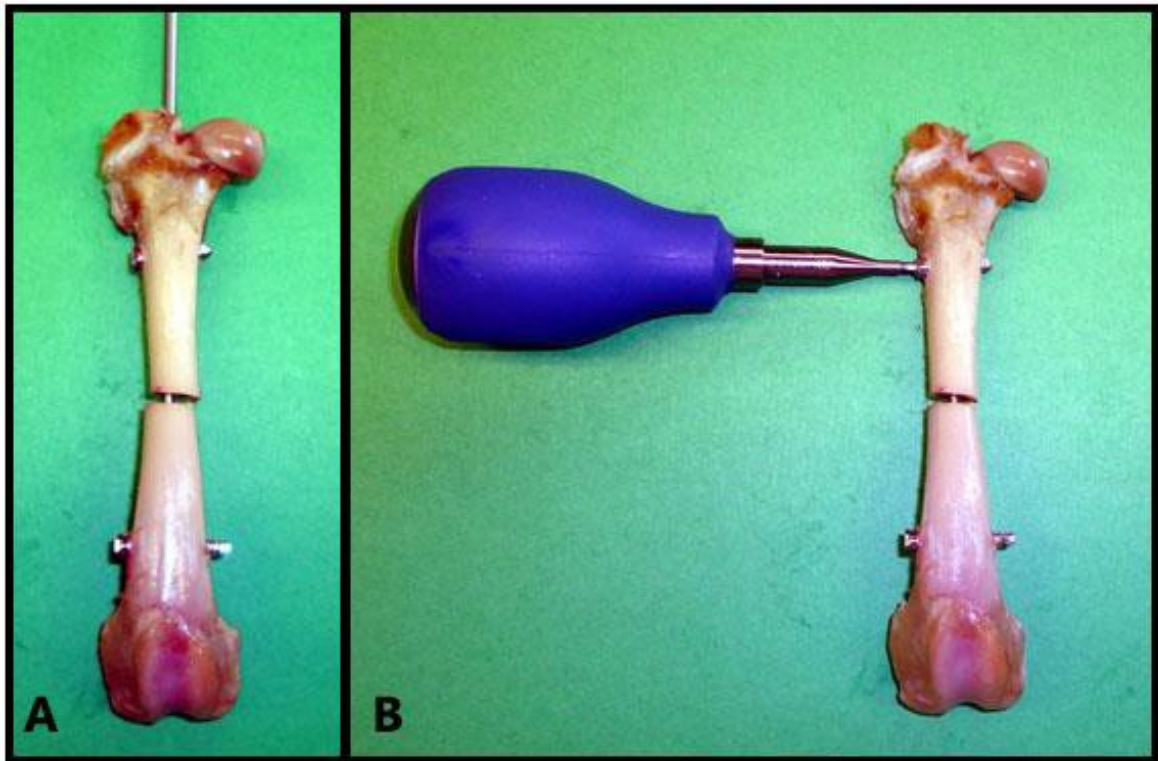


Figure 11. A) Picture of a canine right femur from group 1 with both screws in position and the intramedullary nail inserted. B) Picture of the same femur after the tip of the nail that remained outside of the bone was cut. Fixing screws were inserted and locked by use of a special 1.8 Nm torque screwdriver (blue instrument). Guelph, 2014.

Group 2: Femurs were prepared similarly as in Group 1; the only variation was that the proximal locking screw was placed in a location equidistant between the proximal mark and the osteotomy, resulting in a 25% shorter inter-bolt distance (Figure 12).



Figure 12. A) Canine right femur from group 2. After the points were marked, the distance between them was measured (X), and the midpoint was defined as the osteotomy line. The midpoint between the first landmark and the osteotomy line was set to be the hole for the proximal screw (black dot). B) Canine right femur from group 2 with TVS in place. Guelph, 2014.

Group 3: Twelve 7-hole LC-DCP® plates, 2.4mm thick each were applied to the lateral aspect of the bones according to the AO/ASIF principles after osteotomy was performed (Figure 13). They were fixed to the bone with six 2.4 mm bicortical screws each, 18 to 22mm long. The plate was positioned so that its middle was located on the 2 mm gap, and the middle shaft was determined after the same landmarks as groups 1 and 2 were determined. The middle hole of the plate was left empty and all the screws were applied in neutral position.

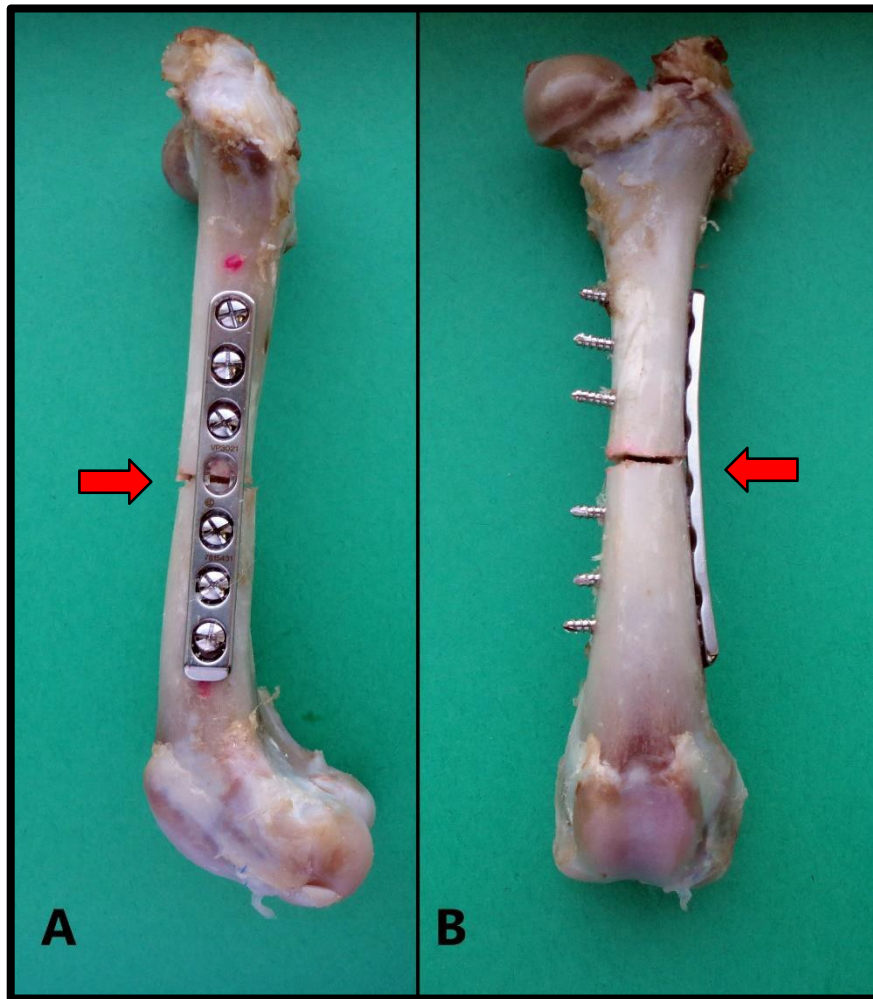


Figure 13. Canine left femur from Group 3 with a 7-hole LC-DCP® plate laterally applied with the middle hole left empty at the osteotomy level (red arrow). A) Lateral aspect. B) Cranial aspect. Guelph, 2014.

Accurate positioning of implants was confirmed radiographically in all specimens (Figures 14 and 15). All specimens were implanted by the same investigator.

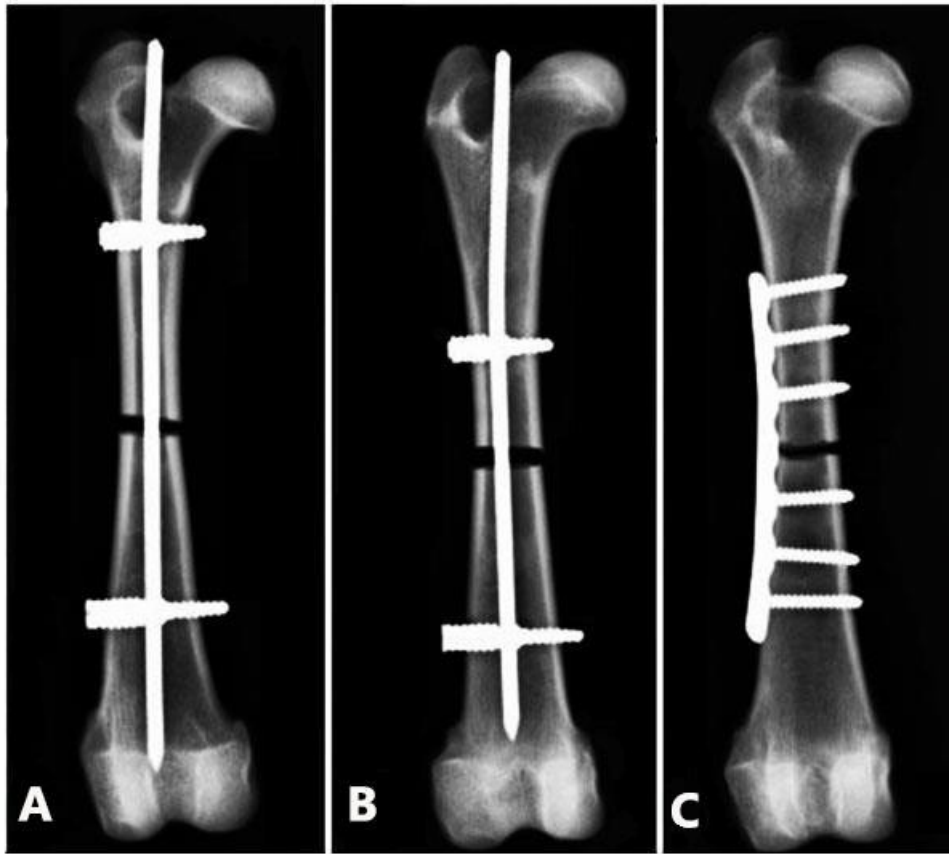


Figure 14. Craniocaudal radiographs used to ascertain correct positioning of the implants. A) Right specimen from group 1 (long nail) with the TVS in place. B) Right specimen from group 2 (short nail) with the TVS in place. C) Right specimen from group 3 with the plate and screws in position. Guelph, 2014.

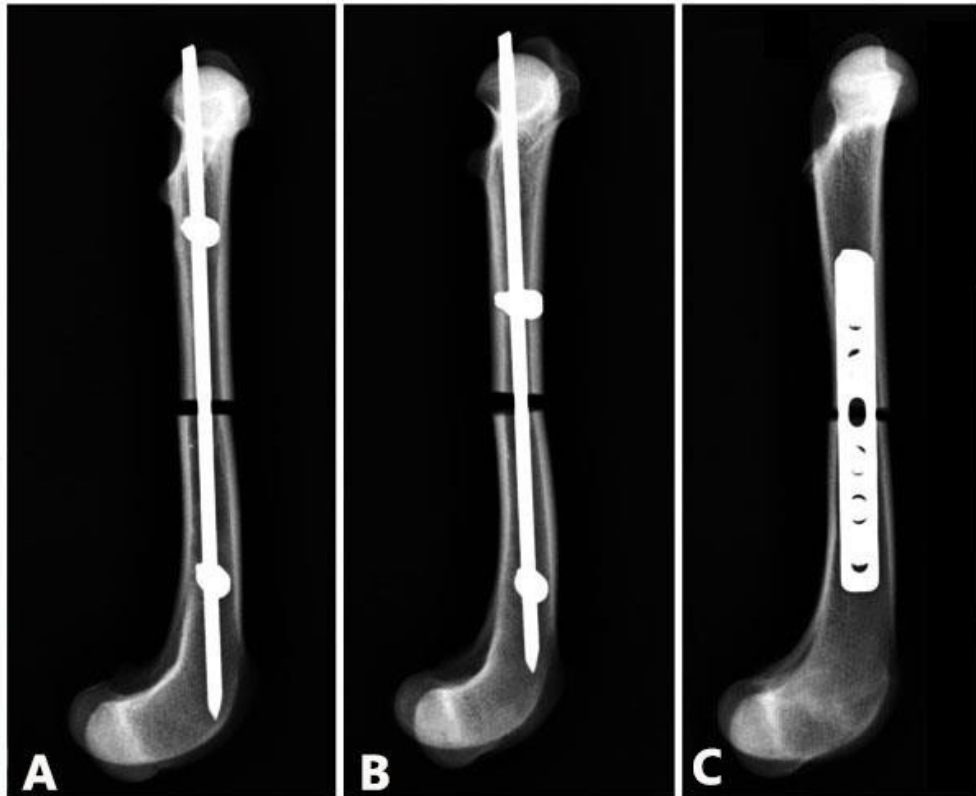


Figure 15. Latero-medial radiographs used to ascertain correct positioning of the implants. A) Right specimen from group 1 (long nail) with the TVS in place. B) Right specimen from group 2 (short nail) with the TVS in place. C) Right specimen from group 3 with the plate and screws in position. Guelph, 2014.

4.5 Biomechanical analysis

The cranial and distal parts of the femurs were embedded in casting epoxy resin West System 105/205 Epoxy Resin⁵ with hardener, with care not to include the implants on the casting inside steel cubes (Figure 16).

⁵ West System, Bay City, Michigan, USA.

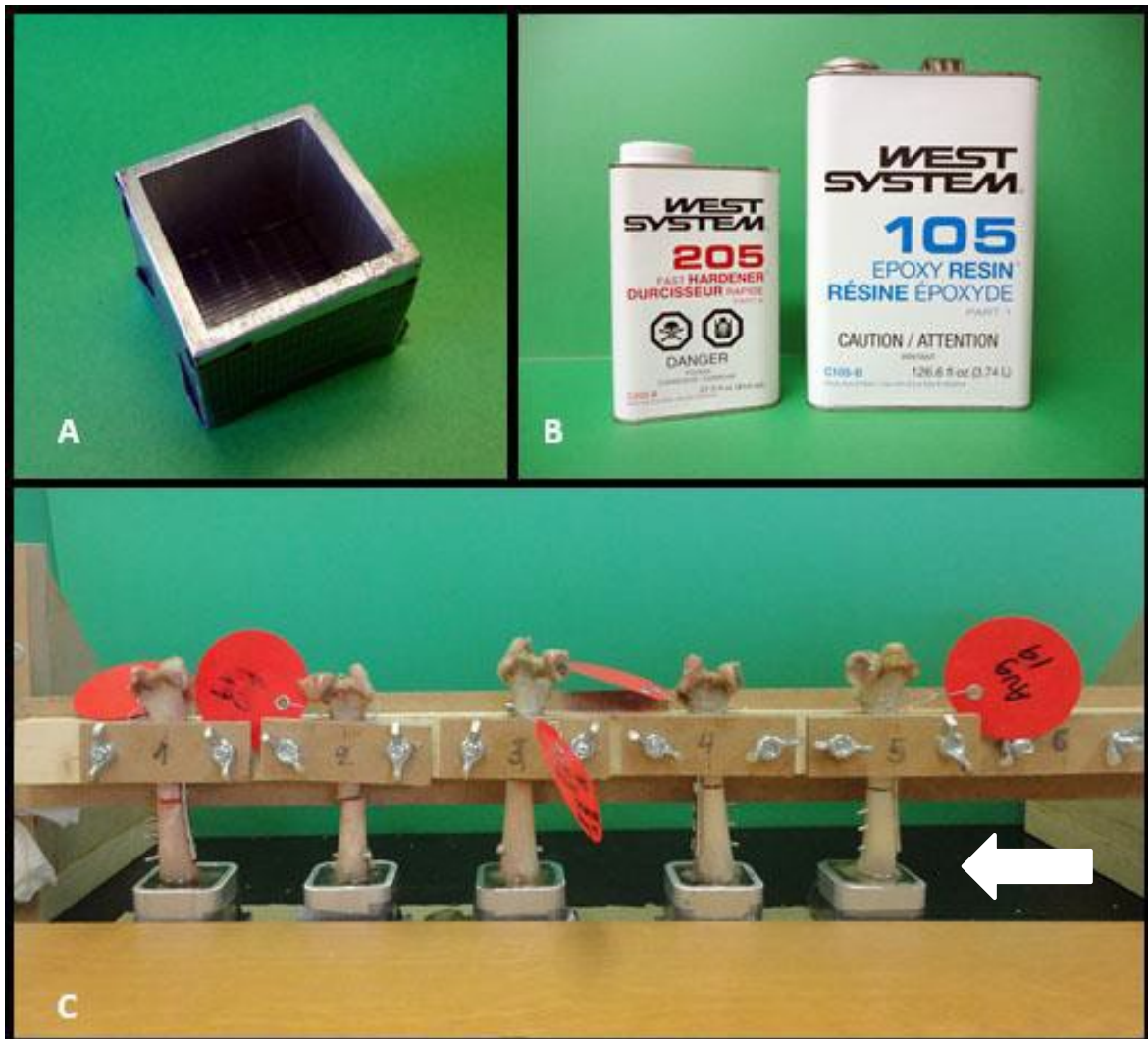


Figure 16. A) Steel cube of 2.5 x 2.5 X 2 cm used for positioning bones for potting. Duct tape was placed along the cube's base to prevent the epoxy from leaking out of the cube. B) Epoxy resin West System 105/205 Epoxy Resin® with hardener. C) Custom-made potting fixture Note bones with the distal epiphyses embedded in epoxy resin (white arrow). Guelph, 2014.

After prepared, constructs were securely mounted in a custom designed torsion jig (Figure 17) that ensured accurate axial alignment and testing length pattern for all specimens. Moisture of all specimens was maintained throughout the preparation process and biomechanical testing by use of isotonic saline solution.

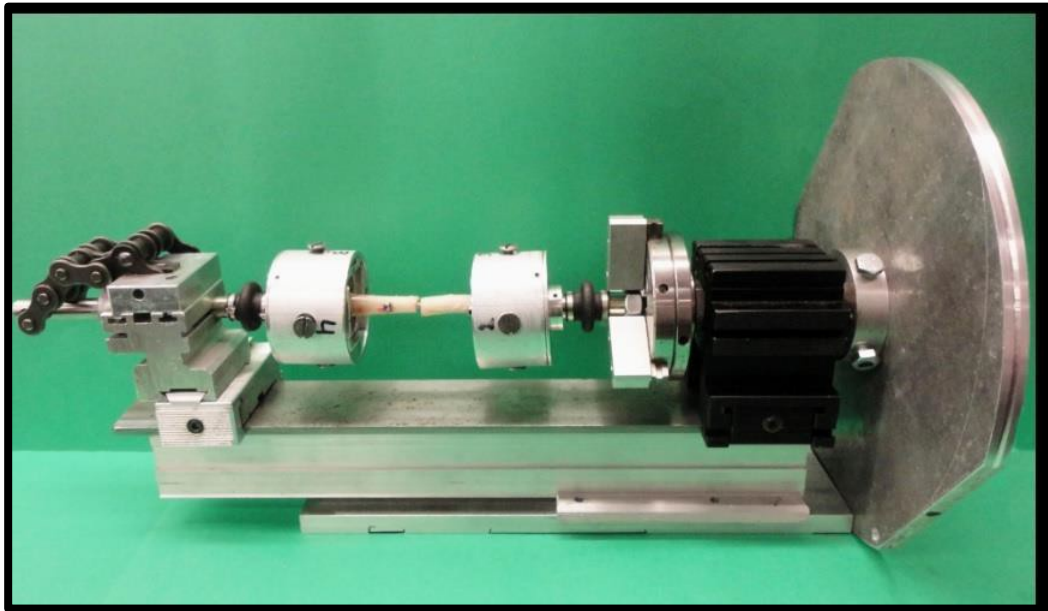


Figure 17. Custom designed torsion jig with specimen from group 2 (short nail). Guelph, 2014.

The torsion jig was linked to a 130-mm-radius wheel and fastened to a metal bar connected to a testing machine⁶ (Instron® Model #5965) with a 0.5 kN load cell by a block with pivot (Figure 18-A). For the load to failure test the metal bar was removed and a wire cable was attached to the loading wheel and tension was then applied until implant or bone failure (Figure 18-B).

⁶ Instron Canada Inc., Burlington, ON, CA.

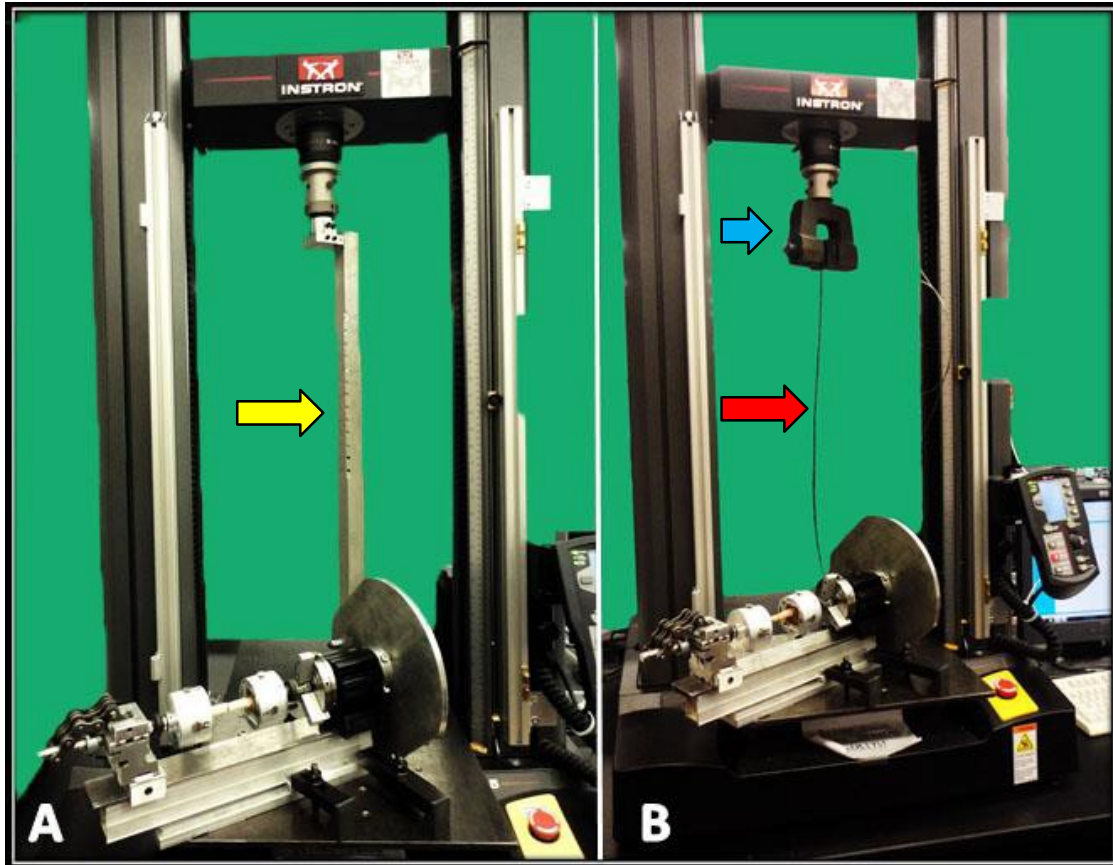


Figure 18. A) Torsion fixture attached to the Instron universal testing machine connected to a 0.5 kN load cell by a metal bar (yellow arrow), with bone sample ready for non-destructive cyclic load torsion test. B) Torsion wheel attached to a wire cable (red arrow) connected to the load cell by a block with pivots (blue arrow), for load to failure test. Guelph, 2014.

A load to failure test was performed for each group to determine the maximum torque the implants resisted, in order to test approximately 70% of the maximum reached for cyclic tests (± 0.57 Nm).

4.5.1 Data acquisition

The jig allowed 5 degrees of freedom but controlled for torque in the axial direction. The samples were tested non-destructively at a rate of $1^\circ/\text{sec}$ under load control between a torque of ± 0.57 Nm for 10 cycles in accordance with a protocol

previously described (VON PFEIL et al., 2005). Cyclic loading was followed by an acute torsion to failure at a similar rate. Data was acquired at 50 Hz. The last of the 10 cycles was used to measure the deformation under non-destructive load. A data acquisition software (Labview⁷) was used. Cyclic tests were repeated with a rigid body (aluminium bar) to discard any machine looseness (slack).

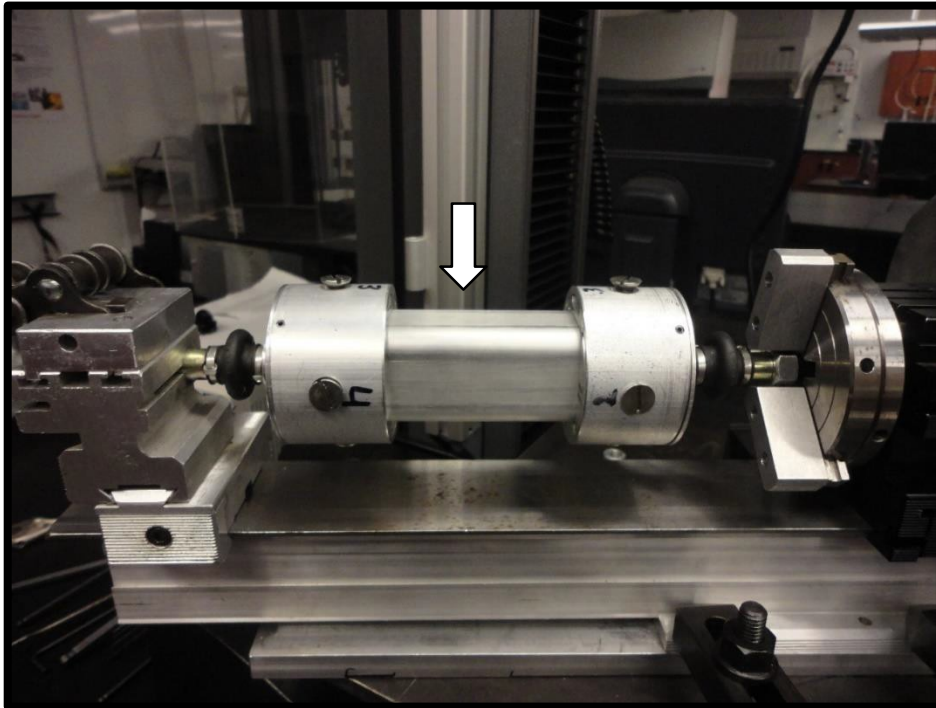


Figure 19. Torsion jig with an aluminium bar (white arrow) before test. Guelph, 2014.

The amount of deformation of a rigid body subjected to the same loading conditions was subtracted from the deformation of the samples to account for slack in the jig.

Stiffness and torque to failure of the constructs were measured from the final torque-deformation curves. Stiffness was defined as the slope of the straight portion of the load/deformation curves ($y=ax+b$), where stiffness was represented as “a” by linear

⁷ National Instruments, Mississauga, ON, CA.

regression. Yield point was defined as the torque resulting in a 1° deformation beyond the expected linear behavior of the constructs.

Compliance was measured as the displacement under cyclic load on the last cycle on +/- 0.57 Nm.

Torsional load ***M*** for load to failure test, in ***Nm***, was calculated by the formula:

$$M = F \cdot R$$

Where ***F*** is the load applied by the machine in ***N*** and ***R*** is the radius of cable from center of tester in ***m***.

Torsional load ***M*** for cyclic test was in ***Nm***, calculated by the formula:

$$M = F \cdot \sin (\sin^{-1}(\text{displacement}/R)+90)$$

Where ***F*** is the load applied by the machine in ***N***, ***displacement*** stands for the crosshead displacement from the level position on the wheel, in ***m***, and ***R*** is the radius of bolt to loading wheel center in ***m***.

4.6 Statistical analysis

All parameters were tested for normality using a Shapiro-Wilk test and examination of the residuals. Data was compared using three-way ANOVA accounting for the random effect of “dog” and distance between bolts, and bone diameter as co-variables. Post-hoc adjustments were made using Tukey test when significant differences were found, P values < 0.05 were considered significant. Statistical analyses were conducted with commercial statistical software⁸ (SAS/STAT Version 8).

⁸ SAS Institute Inc., Cary, NC, USA.

5. RESULTS

5.1 Specimens

Femurs collected for the study were homogeneous in size, despite different breed origin. Mean \pm SD of femoral length was 109.3 \pm 5.9 mm with mean width of the femoral medullary cavity at the mid-diaphysis 9.5 \pm 0.7 mm. All bones had a diameter larger than 8.5 mm at the bolt location, in accordance to previous recommendations made for the TVS (BRÜCKNER; UNGER; SPIES, 2014). For each bone pair, there was not disparities between the left and the right side specimens. Bone diameter was measured in three landmarks (1- just below the lesser trochanter; 2- on the mid-diaphysis; 3- on the point just above the fabellae). Table 1 shows length and width distribution:

Table 1. Bone's measurements. LesserT width = medullary width at the Lesser Trochanter landmark in mm. MidS width = medullary canal width at the midshaft landmark in mm. Fabellae width = medullary canal width on the imaginary point just above the Fabellae in mm. Guelph, 2014.

Bone nº	Group nº	Length	LesserT width	MidS width	Fabellae width
4	1	103	12	8.5	15
6	1	112	12.5	10.5	16.5
7	1	112.5	11.5	10	17.5
14	1	100	10.5	9	16.5
17	1	107	12	9	17
24	1	111	13.5	10.5	18.5
27	1	105.5	10.5	9	14
31	1	106	14	10	17
32	1	110	11	10	17
34	1	115	13.5	10	17
35	1	115	11.5	9.5	17.5
38	1	110.5	13.5	9.5	18
2	2	107.4	12	8.5	16
5	2	101	11.5	9	14.5

8	2	121	10	8.5	14
15	2	115	13	11	18
16	2	107.5	12	8.5	17.5
18	2	106	12	8.5	16
19	2	107	12	9.5	16
23	2	110	12	9	16.5
26	2	124	11.5	9.5	14.5
29	2	107.5	11	8.5	17.5
36	2	101.5	11.5	10	16.5
37	2	121	14.5	10.5	17.5
3	3	111	12.5	9.5	16.5
9	3	104	13	9.5	17
11	3	109.5	12.5	10	17
12	3	109.5	11.5	10	17.5
13	3	115	14.5	10.5	19.5
20	3	102.5	11	9	13
21	3	97.5	10	8.5	13.5
25	3	105	12	10.5	16.5
28	3	107.5	13	9	16
30	3	110	12.5	9.5	17
33	3	114.5	13.5	10	17.5
39	3	114.5	14.5	9.5	19.5

Table 2. Mean +/- SD of bone's measurements distribution between groups. LesserT width = medullary width at the Lesser Trochanter landmark in mm. MidS width = Medullary canal width at the midshaft landmark in mm. Fabellae width = Medullary canal width on the imaginary point just above the Fabellae in mm. Guelph, 2014.

Group	Length	LesserT Width	MidS Width	Fabellae width
1	109 +/- 4.7	12.1 +/- 1.2	9.7 +/- 0.7	16.8 +/- 1.2
2	110.1 +/- 7.7	12 +/- 1.1	9.2 +/- 0.8	16.2 +/- 1.3
3	108.4 +/- 5.3	12.5 +/- 1.3	9.6 +/- 0.6	16.7 +/- 1.9

5.2 Torsion tests

5.2.1 Cyclic loading

Compliance curves in torsion had different behaviour and were unimodal for the nails (groups 1 and 2) and bimodal for group 3 (plates). The rigid bar did not show displacement under test. The different types of curves obtained in cyclic loading tests are represented in the following graph (Figure 20).

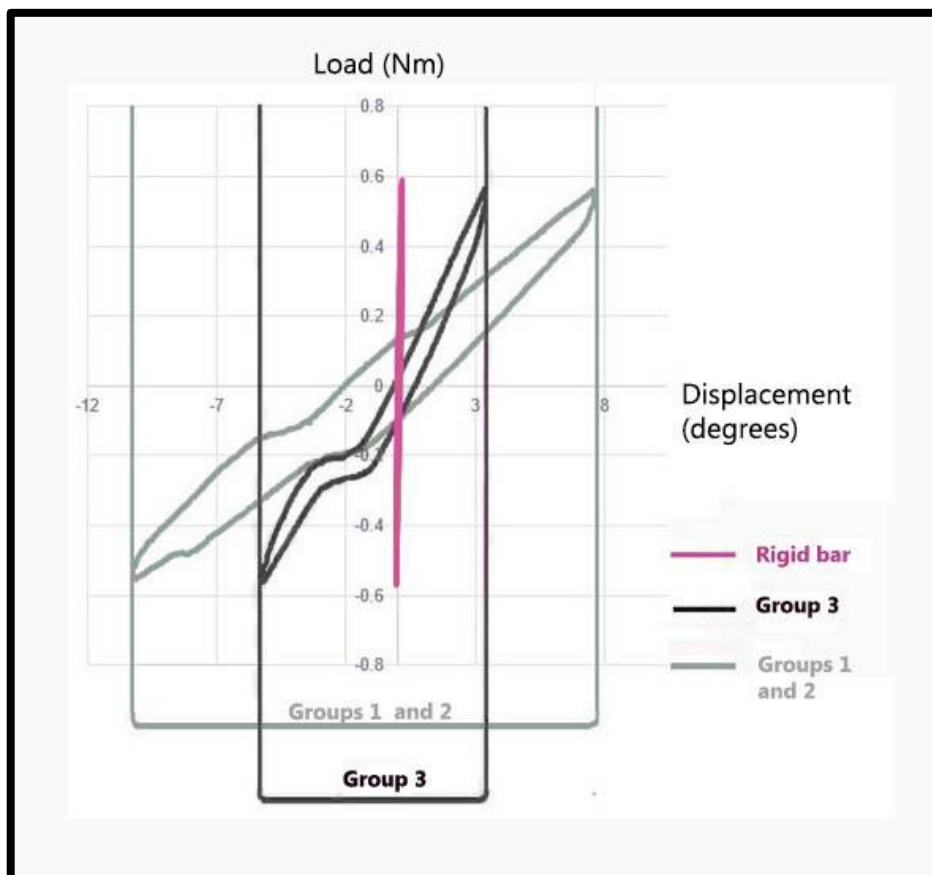


Figure 20. Schematic graph representing an example of the load/displacement curves for groups 1 and 2 (TVS nails) (light grey line), for group 3 (plates) (dark grey line) and the rigid steel bar (pink line) on cyclic tests. Guelph, 2014.

5.2.1.1 Compliance

There was no significant statistic difference between groups 1 and 2 for

compliance (displacement under cyclic load), but there was significant difference between group 3 and groups 1 and 2.

Table 3. Comparison of means and standard deviations (SD) of all groups for compliance after cyclic loading test. Different letters show significant statistic difference on Tukey test at 5% confidence level. Guelph, 2014.

Group	Mean	SD
1	16.59 a	+/- 2.54
2	15.61 a	+/- 2.12
3	7.85 b	+/- 1.064

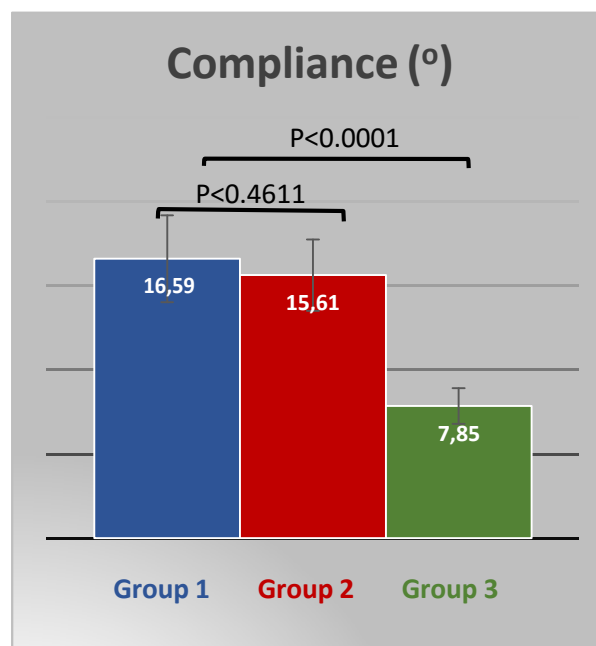


Figure 21. Bar chart representing means and SD compliances of all groups. Group 1 (Long nail- blue), group 2 (Short nail - red) and group 3 (plates - green). Guelph, 2014.

5.2.2 failure

On single load to failure, yield point was determined as one degree of deformation beyond the expected linear behavior.

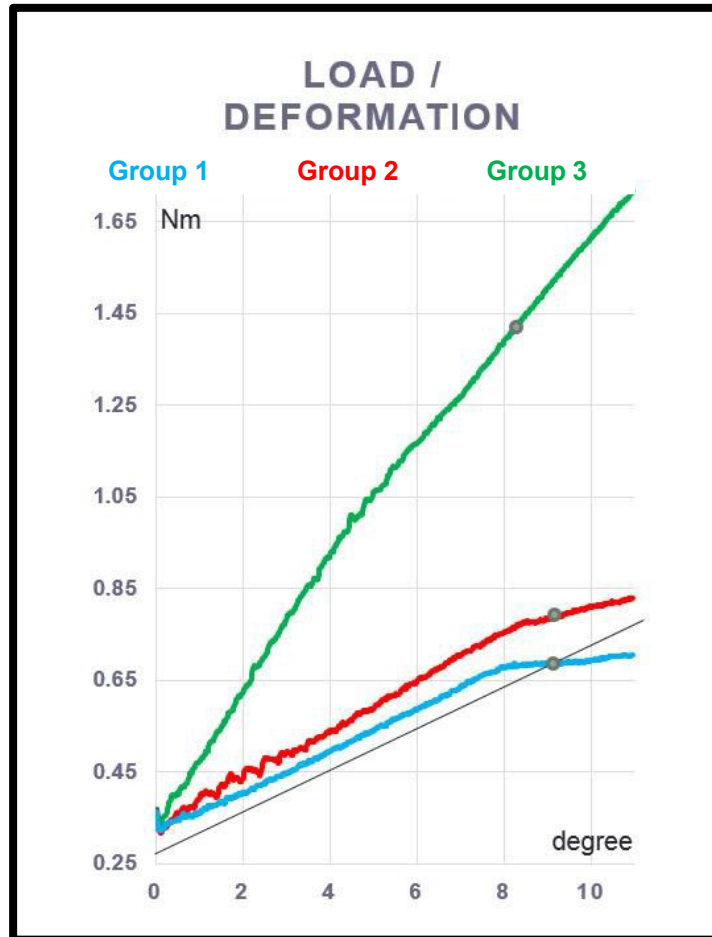


Figure 22. Schematic graph representing examples of load/displacement curves of all groups: Group 1 Long nail (blue), group 2 Short nail (red) and group 3 plates (green). The grey line and dots indicate the yield point calculated by linear regression. Guelph, 2014.

5.2.2.1 Yield Torque

There was no significant statistical difference between groups 1 and 2 for yield torque, but there was significant difference between group 3 and groups 1 and 2.

Table 4. Comparison of means and standard deviations (SD) of all groups for yield torque after load to failure test. Different letters show significant statistic difference on Tukey test at 5% confidence level. Guelph, 2014.

Group	Mean (Nm)	SD
1	0.8055 a	+/- 0.1833
2	0.8054 a	+/- 0.0938
3	1.7367 b	+/- 0.4609

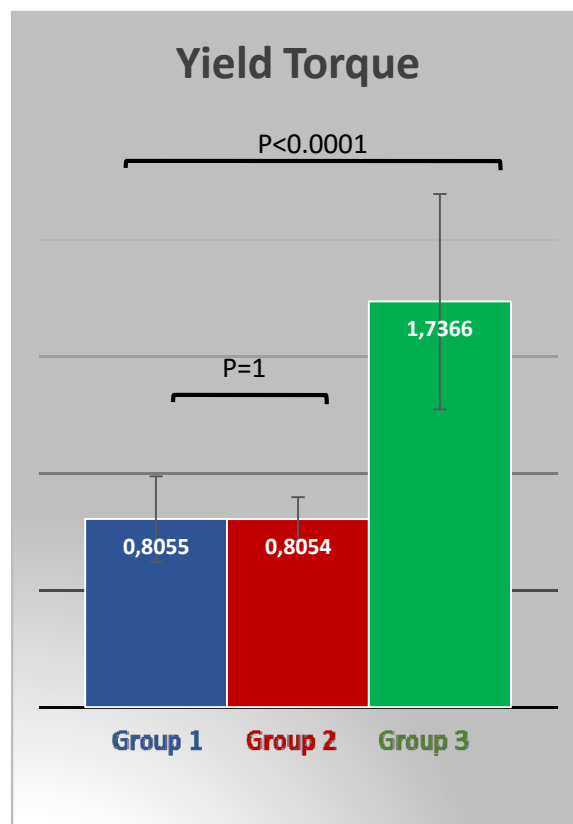


Figure 23. Bar chart representing means and SD for torque at yield of all groups. Group 1 (blue), group 2 (red) and group 3 (green). Guelph, 2014.

5.2.2.2 Stiffness

There was no significant statistic difference between groups 1 and 2 for stiffness, but there was significant difference between group 3 and groups 1 and 2.

Table 5. Comparison of means and standard deviations (SD) of all groups for stiffness after load to failure test. Different letters show significant statistic difference on Tukey test at 5% confidence level. Guelph, 2014.

Group	Mean (Nm/deg)	SD
1	0.0502 a	+/- 0.010
2	0.0583 a	+/- 0.006
3	0.1409 b	+/- 0.014

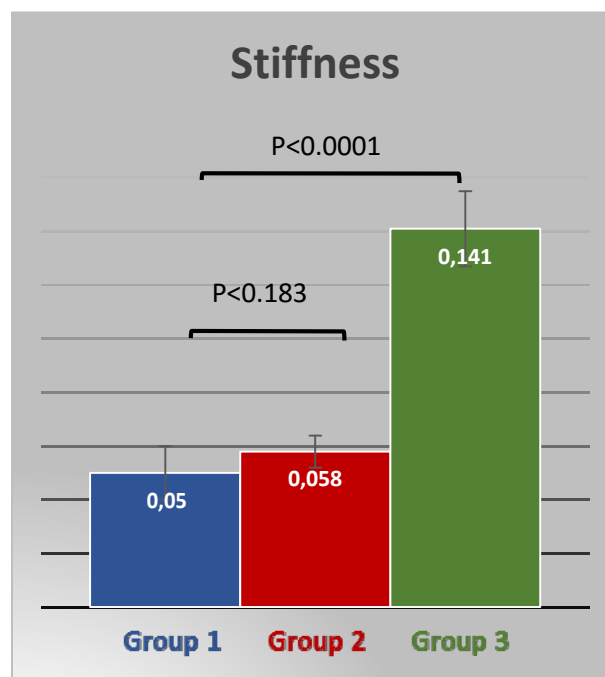


Figure 24. Bar chart representing means and SD for stiffness of all groups. Group 1 (blue), group 2 (red) and group 3 (green). Guelph, 2014.

Table 6. Tests results of all groups. “Bolt dist” = distance between bolts for groups 1 and 2. For group 3 the distance considered was the length of the plates. “Stiff” = Torsional Stiffness, “Yield’ = Torque at Yield, “Compliance’ = Displacement under cyclic loading. Guelph, 2014.

Bone nº	Group	Bolt dist (mm)	Stiff (Nm/°)	Yield (Nm)	Compliance (°)
4	1	64.2	0.0418	1.02	18.8
6	1	60.5	0.044	1.0723	14.4
7	1	60.5	0.0473	1.0243	12.8
14	1	58	0.0536	0.6652	14.3
15	1	55.4	0.049	0.8109	18.6
17	1	55.5	0.0465	0.6769	14.5
24	1	59	0.0461	0.6282	20.0
27	1	57	0.0742	0.9005	13.6
31	1	56	0.0668	0.4652	18.3
32	1	56	0.0498	0.8903	17.3
35	1	60	0.0416	0.7447	19.4
38	1	51.5	0.0424	0.7675	17.4
2	2	44.15	0.0564	0.9061	18.6
5	2	41.1	0.0517	0.7343	16.3
8	2	49	0.0484	0.7342	20.2
16	2	35.5	0.054	0.8972	15.8
18	2	36	0.0614	0.6006	13.1
19	2	42	0.051	0.8359	14.9
23	2	45	0.0644	0.9478	14.3
26	2	51.5	0.0554	0.7957	15.7
29	2	45	0.066	0.7864	14.5
34	2	48.5	0.0579	0.8291	15.1
36	2	34	0.0695	0.8441	12.6
37	2	45.5	0.0637	0.7542	16.1
3	3	57	0.1406	2.3267	6.8
9	3	57	0.1524	2.2977	5.8
11	3	57	0.1359	2.0304	8.1
12	3	57	0.1553	2.4369	7.5
13	3	57	0.1574	1.5649	7.2
20	3	57	0.1522	1.3612	7.6
21	3	57	0.1493	1.0892	7.6
25	3	57	0.127	1.622	8.0
28	3	57	0.1283	1.1914	8.4
30	3	57	0.1228	1.6188	9.0
33	3	57	0.1161	1.9414	10.0
39	3	57	0.1542	1.3597	8.2

Table 7. Mean +/- SD of all groups. "Bolt dist" = distance between bolts for groups 1 and 2. For group 3 the distance considered was the length of the plates. "Stiff" = Torsional Stiffness, "Yield" = Torque at Yield, "Compliance" = Displacement under cyclic loading. Different letters show significant statistic difference on Tukey test at 5% confidence level. Guelph, 2014.

Group	Bolt dist (mm)	Stiff (Nm/°)	Yield (Nm)	Compliance (°)
1	57.8 +/- 3.3	0.05 +/- 0.01 a	0.806 +/- 0.183 a	16.59 +/- 2.54 a
2	43.1 +/- 5.6	0.05 +/- 0.007 a	0.805 +/- 0.094 a	15.61 +/- 2.12 a
3	57 +/- 0	0.14 +/- 0.015 b	1.737 +/- 0.461 b	7.85 +/- 1.06 b

There was no bone fracture during tests; just one of the specimens from group 3 (bone n° 11) suffered a small fissure while drilling one screw hole to fix the plate but the plate was held in position. All implants were retrieved (Figure 25) after tests and the TVS bolts did not show any structural damage. All the TVS nails, however, presented elongated marks left by the locking mechanism of the fixing screws on the rod suggesting slippage of one of the two screws.

All plates had signs of wear consisting of flattening of the screw threads, structural damage to the edges of the screw holes and bending.

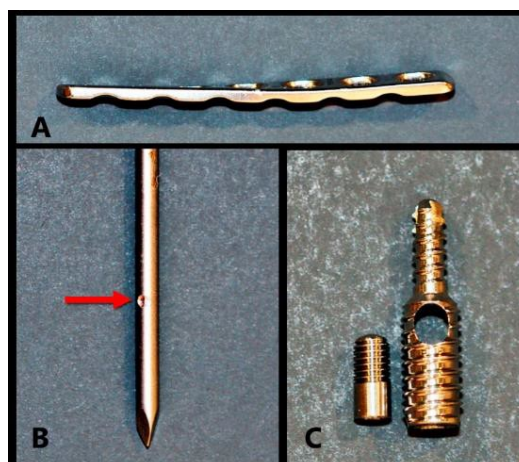


Figure 25. Implants retrieved after load to failure tests. A) A 2.4 mm LC-DCP® plate

bent after test. B) A 2.5 mm nail with an elongated mark left by the locking mechanism of the bolts after the test (red arrow). C) A 16 mm TVS bolt and fixing screw without any structural damage, retrieved after test. Guelph, 2014.

8. DISCUSSION

Our results show that the 2.5 mm TVS system has only half the torsional strength and approximately a third of the stiffness of a 2.4 mm LC-DCP plate in a 2 mm mid-shaft open gap fracture canine model in torsion. To our knowledge there has not been another study published addressing the torsional properties of the TVS so far. This result cannot be extrapolated to all forces acting on the living animal. On a study conducted by Brückner et al. (2014), the TVS was compared to a 2.0 dynamic compression plate (DCP) in an osteotomy gap model under shear forces applying axial force on a 21° angle with feline femoral heads. They concluded that under this vector of force, the TVS is at least comparable to DCP plate. Torsion is naturally induced on normal weight bearing and can be very complex to assess (ROE, 1998).

The same study concluded that the minimum required bone diameter to safely insert bolts in feline bones was 8.5 mm. Based on that finding, we aimed to perform a study with feline femurs, but we had a major problem finding euthanized animals with the minimum required bone size. The smallest cat on that study had a proximal femur diameter of 11 mm and 13 mm distally. We had similar numbers but only with small dogs' femurs. That could be explained because the humane societies we had access to may not receive excessive amount of stray cats in Canada, so the sample population is smaller. That bone diameter also represents a limiting factor for the TVS because a 4.8 mm bolt occupies 56% of an 8.5 mm bone diameter and surpasses the AO

recommendation that the diameter of bicortical screws should not exceed 20-25% of the bone diameter, situation that could enhance the risk of fractures on the screw hole (GIBSON et al., 2008).

Because large cortical holes increase the risk of failure of bone in torsion, we expected that the nail constructs would fail by fracture of the bone. That did not occur in any of the nail constructs and may be the result of failure of the gripping mechanism of the TVS. Although the study conducted by Brückner et al. (2014) concluded that the single larger hole on bone is statistically more resistant than the six holes created by the 2.0 mm cortical screws on feline bone. It must be noted that the potting epoxy was generally 1 cm away from the location of the bolt and could have increased bone resistance to fracture on our study.

An implant's characteristics such as diameter, material properties, wall thickness, curvature and cross-sectional shape are determinant for their mechanical properties (KINAST; FRIGG; PERREN, 1990). For a cylindrical rod, torsional stiffness is inversely proportional to length. (MUIR; JOHNSON; MARKEL, 1995). We expected an increase in stiffness of the constructs in group 2 because in this group the nail was 25% shorter than group 1. The lack of interaction between bolt distance and stiffness was unexpected but may indicate that the system does not behave as a completely locked system. Instead, it suggests that the stiffness of the system may be more dependent on the quality of the bolt gripping mechanism on the rod rather than determined by the properties of the rod itself. The latter is also supported by the large displacement observed under cyclic loading and the elongated marks left by the locking mechanism of the bolts on the rod suggesting slippage of one of the 2 bolts on the rod during testing. Torsional instability on interlocking nail is a result of the

discrepancy between the nail hole diameter and the diameter of the bolt and this effect may be exacerbated under torsion (VON PFEIL et al., 2005). In this case, that could be a discrepancy between screw hole diameter and nail diameter, with slippage. Interlocking nails show weakness at the screws holes because the locking screws or bolts do not interact rigidly with the nail and therefore do not help to reduce the stresses as they would on a locking compression plate (APER et al., 2003). In this case, there was no rigid interaction either.

It has been suggested that implant failure could occur on the intersection of the thinner and the thicker parts of the locking bolts due to stress rising (Brückner et al. 2014) but we did not have such type of failure. The early designed veterinary ILNs had stress concentrated on the nails holes due to local decrease in Area Moment of Inertia, and usually failed on those points (DUELAND et al. 1997). The weakest point on a regular interlocking nail is the screw hole, not diminished by the placement of a screw on such hole (ROE, 1998). The holes act as stress concentrators and may result in fatigue failure of the screw or bolt (DÉJARDIN et al., 2006; REEMS; PLUHAR; WHEELER, 2006). Studies have demonstrated that stress is markedly high at the distal screw of a regular interlocking nail, place of frequent mechanical failure. The extension of contact between the nail and cortical bone, the distance from the distal locking screw and the fracture site, the number of screws on the jig and the length of the locking screw can affect this type of stress (LIN et al., 2001). Dynamic compression plates (DCP) can also undergo excessive cyclic bending on empty screw holes when perfect anatomical reconstruction is not achieved due to its eccentric placement or when there is no transcortical support (VON PFEIL et al., 2005). We applied the plates without compression and with a 2 mm gap, which could have made them weaker in torsion.

This study had some limitations. All implants were applied by the same investigator (A.S.M.), not a board certified surgeon. We tested the implants just in torsion, and that represents only one of the acting forces on the living animal. The results could be very different under compression and bending forces.

7. CONCLUSION

Our hypothesis were not proved. The location of the bolts did not influence the torsional properties nor the ultimate strength of the constructs, probably due to slippage of the system and the 2.5 mm TVS system is weaker than the 2.4 mm LC-DCP plate in torsion. Other forces that act on the living animal should be measured *in vitro* so that recommendations can be made for clinical tests.

8. REFERENCES

AN, Y.; BARFIELD, W.; DRAUGHN, R. Basic concepts of mechanical property measurement and bone biomechanics. In: AN, Y.; DRAUGHN, R. (Eds.). **Mechanical Testing of Bone and the Bone-implant Interface**. 1st. ed. Boca Raton: CRC Press, 2000. p. 23–40.

APER, R.L.; LITSKY, A.S.; ROE, S.C.; JOHNSON, K.A. Effect of bone diameter and eccentric loading on fatigue life of cortical screws used with interlocking nails. **American Journal of Veterinary Research**, v. 64, n. 5, p. 569–573, 2003.

ARON, D.N.; JOHNSON, A.L.; PALMER, R H. Biologic strategies and a balanced concept for repair of highly comminuted long bone fractures. **The Compendium on Continuing Education for the Practicing Veterinarian**, v.17, n.1, p. 35-49. 1995.

ATHANASIOU, K.A.; ZHU, C.; LANCTOT, D.R; AGRAWAL, C.M.; WANG, X. Fundamentals of biomechanics in tissue engineering of bone. **Tissue Engineering**, v. 6, n. 4, p. 361–381, 2000.

AUGAT, P.; SIMON, U.; LIEDERT, A.; CLAES, L. Shear movement at the fracture site delays healing in a diaphyseal fracture model. **Journal of Orthopaedic Research**, v. 21, n. 6, p. 1011–1017, 2003.

AUTEFAGE, A. The point of view of the veterinary surgeon: bone and fracture. **Injury**, v. 31 n. 3, p. 50–55, 2000.

BASINGER, R.R.; SUBER, J.T. Two techniques for supplementing interlocking nail repair of fractures of the humerus, femur, and tibia: Results in 12 dogs and cats. **Veterinary Surgery**, v. 33, n. 6, p. 673–680, 2004.

BERGER, L.; FISCHERAUER, S.; WEIß, B.; CELAREK, A.; CASTELLANI, C.; WEINBERG, A.; TSCHEGG, E. Unlocked and locked elastic stable intramedullary nailing in an ovine tibia fracture model: A biomechanical study. **Materials Science and Engineering: C**, v. 40, p. 267–274, 2014.

BERNARDE, A.; DIOP, A.; MAUREL, N.; VIGUIER, E. An in vitro biomechanical comparison between bone plate and interlocking nail. **Veterinary and Comparative Orthopaedics and Traumatology**, v. 15, n. 2, p. 57-66, 2002.

BONIN, G.A.; BAKER, S.T.; DAVIS, C.A.; BERGERSON, C.M.; HILDEBRANDT, A.A.; HULSE, D.A.; KERWIN, S.C.; MORENO, M.R.; SAUNDERS, W.B. In Vitro Biomechanical Comparison of 3.5 mm LC-DCP/Intramedullary Rod and 5 mm Clamp-Rod Internal Fixator (CRIF)/Intramedullary Rod Fixation in a Canine Femoral Gap Model. **Veterinary Surgery**, v. 43, n. 7, p. 860-868, 2014.

BONUCCI, E. Basic composition and structure of bone. In: IN: AN, Y. H., DRAUGHN, R. A. (Ed.). **Mechanical Testing of Bone and the Bone-implant Interface**. 1st. ed. Boca Raton: CRC Press, 2000. p. 3–21.

BRÜCKNER, M.; UNGER, M.; SPIES, M. In vitro biomechanical comparison of a newly designed interlocking nail system to a standard DCP. Testing of cat femora in an osteotomy gap model. **Tierärztliche Praxis. Ausgabe K, Kleintiere/Heimtiere**, v. 42, n. 2, p. 79–87, 2014.

BURNS, C.G.; LITSKY, A.S.; ALLEN, M.J.; JOHNSON, K.A. Influence of Locking Bolt Location on the Mechanical Properties of an Interlocking Nail in the Canine Femur. **Veterinary Surgery**, v. 40, n. 5, p. 522–530, 2011.

DAILEY, H.L.; DALY, C.J.; GALBRAITH, J.G.; CRONIN, M.; HARTY, J.A. A novel intramedullary nail for micromotion stimulation of tibial fractures. **Clinical Biomechanics**, v. 27, n. 2, p. 182–188, 2012.

DAILEY, H.L.; DALY, C.J.; GALBRAITH, J.G; CRONIN, M.; HARTY, J.A. The Flexible Axial Stimulation (FAST) intramedullary nail provides interfragmentary micromotion and enhanced torsional stability. **Clinical Biomechanics**, v. 28, n. 5, p. 579–585, 2013.

DÉJARDIN, L.M.; LANSDOWNE, J.L.; SINNOTT, M.T.; SIDEBOTHAM, C.G.; HAUT, R.C. In vitro mechanical evaluation of torsional loading in simulated canine tibiae for a novel hourglass-shaped interlocking nail with a self-tapping tapered locking design. **American Journal of Veterinary Research**, v. 67, n. 4, p. 678–685, 2006.

DÉJARDIN, L.M.; CABASSU, J.B.; GUILLOU, R.P.; VILLWOCK, M.; GUIOT, L.P.; HAUT, R.C. In vivo biomechanical evaluation of a novel angle-stable interlocking nail design in a canine tibial fracture model. **Veterinary Surgery**, v. 43, n. 3, p. 271–281, 2014.

DÉJARDIN, L.M.; GUIOT, L.P.; VON PFEIL, D.J.F. Interlocking Nails and Minimally Invasive Osteosynthesis. **Veterinary Clinics of North America - Small Animal Practice**, v. 42, n. 5, p. 935–962, 2012.

DÍAZ-BERTRANA, M.C.; DURALL, I.; PUCHOL, J.L.; SÁNCHEZ, A.; FRANCH, J. Interlocking nail treatment of long-bone fractures in cats: 33 Cases (1995-2004). **Veterinary and Comparative Orthopaedics and Traumatology**, v. 18, n. 3, p. 119–126, 2005.

DUDA, G.N.; ECKERT-HÜBNER, K.; SOKIRANSKI, R.; KREUTNER, A.; MILLER, R.; CLAES, L. Analysis of inter-fragmentary movement as a function of musculoskeletal loading conditions in sheep. **Journal of Biomechanics**, v. 31, n. 3, p. 201–210, 1997.

DUELAND, R.T.; BERGLUND, L.; VANDERBY, R.; CHAO, E.Y. Structural properties of interlocking nails, canine femora, and femur-interlocking nail constructs. **Veterinary Surgery**, v. 25, n. 5, p. 386–396, 1996.

DUELAND, R.T.; JOHNSON, K.A.; ROE, S.C.; ENGEN, M.H.; LESSER, A.S.

Interlocking nail treatment of diaphyseal long-bone fractures in dogs. **Journal of the American Veterinary Medical Association**, v. 214, n. 1, p. 59–66, 1999.

DUELAND R.T.; VANDERBY R.; MCCABE. R.P. Fatigue Study of Six and Eight mm Diameter Interlocking Nails with Screw Holes of Variable Size and Number. **Veterinary and Comparative Orthopaedics and Traumatology**, v. 10, n. 4, p. 31–36, 1997.

DUHAUTOIS, B. Use of Veterinary Interlocking Nails for Diaphyseal Fractures in Dogs and Cats: 121 Cases. **Veterinary Surgery**, v. 32, n. 1, p. 8–20, 2003.

DURALL, I.; DIAZ, M.C. Early experience with the use of an interlocking nail for the repair of canine femoral shaft fractures. **Veterinary Surgery**, v. 25, n. 5, p. 397–406, 1996.

DURALL, I.; DIAZ, M.C.; MORALES, I. An Experimental Study of Compression of Femoral Fractures by an Interlocking Intramedullary Pin. **Veterinary and Comparative Orthopaedics and Traumatology**, v. 6, n. 2, p. 29-35, 1993.

DURALL, I.; DIAZ, M.C.; MORALES, I. Interlocking Nail Stabilisation of Humeral Fractures: Initial Experience in Seven Clinical Cases. **Veterinary and Comparative Orthopaedics and Traumatology**, v. 7, n. 1, p. 3–8, 1994.

ENDO, K.; NAKAMURA, K.; MAEDA, H.; MATSUSHITA, T. Interlocking intramedullary nail method for the treatment of femoral and tibial fractures in cats and small dogs. **The Journal of veterinary medical science / the Japanese Society of Veterinary Science**, v. 60, n. 1, p. 119–122, 1998.

EVELEIGH, R.J. A review of biomechanical studies of intramedullary nails. **Medical Engineering & Physics**, v. 17, n. 5, p. 323–331, 7 1995.

FRIGG, A.; RILLMANN, P.; PERREN, T.; GERBER, M.; RYF, C. Intramedullary nailing of clavicular midshaft fractures with the titanium elastic nail: problems and complications. **The American journal of sports medicine**, v. 37, n. 2, p. 352–359, 2009.

FROST, H. M. A 2003 update of bone physiology and Wolff's law for clinicians. **Angle Orthodontist**, v. 74, n. 1, p. 3–15, 2004.

GAEBLER, C.; STANZL-TSCHEGG, S.; LAUBE, W.; VÉCSEI, V. The fatigue strength of small diameter tibial nails. **Injury**, v. 32, n. 5, p. 401–405, 2001.

GATINEAU, M.; PLANTÉ, J. Ulnar Interlocking Intramedullary Nail Stabilization of a Proximal Radio-Ulnar Fracture in a Dog. **Veterinary Surgery**, v. 39, n. 8, p. 1025–1029, 2010.

GAUTHIER, C.M.; CONRAD, B.P.; LEWIS, D.D.; POZZI, A. In vitro comparison of stiffness of plate fixation of radii from large-and small-breed dogs. **American Journal of Veterinary Research**, v. 72, n. 8, p. 1112–1117, 2011.

GEHR, J.; NEBER, W. HILSENBECK, F.; FRIEDL, W. New concepts in the treatment of ankle joint fractures. The IP-XS (XSL) and IP-XXS (XXSL) nail in the treatment of ankle joint fractures. **Archives of Orthopaedic and Trauma Surgery**, v. 124, n. 2, p. 96–103, 2004.

GIBSON, T.W.G.; MOENS, N.M.M.; RUNCIMAN, R.J.; HOLMBERG, D.L.; MONTEITH, G.M. The biomechanical properties of the feline femur. **Veterinary and Comparative Orthopaedics and Traumatology**, v. 21, n. 4, p. 312–317, 2008.

GOLDZAK, M.; SIMON, P.; MITTLMEIER, T.; CHAUSSEMIER, M.; CHIERGATTI, R. Primary stability of an intramedullary calcaneal nail and an angular stable calcaneal plate in a biomechanical testing model of intraarticular calcaneal fracture. **Injury**, v. 45, n. 1, p. 49–53, 2014.

GRADL, G.; DIETZE, A.; ARNDT, D.; BECK, M.; GIERER, P.; BÖRSCH, T.; MITTLMEIER, T. Angular and sliding stable antegrade nailing (Targon PH) for the treatment of proximal humeral fractures. **Archives of Orthopaedic and Trauma Surgery**, v. 127, n. 10, p. 937–944, 2007.

HORSTMAN, C.L.; BEALE, B.S.; CONZEMIUS, M.G.; EVANS, R. Biological osteosynthesis versus traditional anatomic reconstruction of 20 long-bone fractures using an interlocking nail: 1994-2001. **Veterinary Surgery**, v. 33, n. 3, p. 232–237, 2004.

HUCKSTEP, R. L. Proceedings: An intramedullary nail for rigid fixation and compression of fractures of the femur. **The Journal of Bone and Joint Surgery. British Volume**, v. 57, n. 2, p. 253, 1975.

HUDSON, C.C.; POZZI, A.; LEWIS, D.D. Minimally invasive plate osteosynthesis: applications and techniques in dogs and cats. **Veterinary and Comparative Orthopaedics and Traumatology**, v. 22, n. 3, p. 175–182, 2009.

JEE, W. S. S. Integrated bone tissue physiology: anatomy and physiology. In: COWIN, S. C. (Ed.). **Bone mechanics handbook**. 2nd. ed. Boca Raton: CRC Press, 2001. p. 1–68.

JOHNSON, A. Current concepts in fracture reduction. **Veterinary and Comparative Orthopaedics and Traumatology**, v. 16, n. 2, p. 59, 2003.

JOHNSON, K.; HUCKSTEP, R. Bone remodeling in canine femora after internal-fixation with the Huckstep nail. **Veterinary Radiology**, v. 27, n. 1, p. 27–30, 1986.

KINAST, C.; FRIGG, R.; PERREN, S.M. Biomechanics of the interlocking nail. **Archives of Orthopaedic and Trauma Surgery**, v. 109, n. 4, p. 197–204, jun. 1990.

KLEIN, P.; SCHELL, H.; STREITPARTH, F.; HELLER, M.; KASSI, J.P.; KANDZIORA, F.; BRAGULLA, H.; HAAS, N.P.; DUDA, G.N. The initial phase of fracture healing is specifically sensitive to mechanical conditions. **Journal of Orthopaedic Research**, v. 21, p. 662–669, 2003.

KUHN, S.; APPELMANN, P.; PAIRON, P.; MEHLER, D.; HARTMANN, F.; ROMMENS, P.M. A new angle stable nailing concept for the treatment of distal tibia fractures. **International Orthopaedics**, v. 38, n. 6, p. 1255–1260, 2014a.

KUHN, S.; APPELMANN, P.; PAIRON, P.; MEHLER, D.; ROMMENS, P.M. The Retrograde Tibial Nail: Presentation and biomechanical evaluation of a new concept in the treatment of distal tibia fractures. **Injury**, v. 45, n. 1, p. 81–86, 2014b.

KUNTSCHER, G. B. The Kuntscher method of intramedullary fixation. **The Journal of Bone and joint Surgery. American Volume**, v. 40, n. 1, p. 17–26, 1958.

LARIN, A.; EICH, C.S.; PARKER, R.B.; STUBBS, W.P. Repair of diaphyseal femoral fractures in cats using interlocking intramedullary nails: 12 cases (1996-2000). **Journal of the American Veterinary Medical Association**, v. 219, n. 8, p. 1098–1104, 2001.

LIN, J.; LIN, S.J.; CHEN, P.Q.; YANG, S.H. Stress analysis of the distal locking screws for femoral interlocking nailing. **Journal of Orthopaedic Research**, v. 19, n. 1, p. 57–63, 2001.

MARKEL, M.D.; SIELMAN, E.; RAPOFF, A.J.; KOHLES, S.S. Mechanical properties of long bones in dogs. **American Journal of Veterinary Research**, v. 55, n. 8, p. 1178–83, 1994.

MARSELL, R.; EINHORN, T.A. The biology of fracture healing. **Injury**, v. 42, n. 6, p. 551–5, 2011.

MARTIN, R.; BURR, D.; SHARKEY, N. **Skeletal Tissue Mechanics**. New York: Springer Science & Business Media, 2013. 392p.

MUIR, P.; JOHNSON, K.A. Interlocking intramedullary nail stabilization of a femoral fracture in a dog with osteomyelitis. **Journal of the American Veterinary Medical Association**. v. 209, n. 7, p. 1262-1264, 1996.

MUIR, P.; JOHNSON, K.A.; MARKEL, M.D. Area Moment of Inertia for Comparison of Implant Cross-Sectional Geometry and Bending Stiffness. **Veterinary and Comparative Orthopaedics and Traumatology**, v. 8, n. 3, p. 146–152, 1995.

NANAI, B.; BASINGER, R R. Use of a new investigational interlocking nail supplement in the repair of comminuted diaphyseal tibia fractures in two dogs. **Journal of the American Animal Hospital Association**, v. 41, n. 3, p. 203–208, 2005.

PALMER, R.H. Biological Osteosynthesis. **Veterinary Clinics of North America: Small Animal Practice**, v. 29, n. 5, p. 1171–1185, 1999.

PARK, S.H.; O'CONNOR, K.; MCKELLOP, H.; SARNIENTO, A. The influence of active shear or compressive motion on fracture-healing. **The Journal of Bone and Joint Surgery. American Volume**, v. 80, n. 6, p. 868–878, 1998.

PERREN, S.M. Evolution of the internal fixation of long bone fractures. The scientific basis of biological internal fixation: choosing a new balance between stability and biology. **The Journal of Bone and Joint Surgery. British Volume**, v. 84, n. 8, p. 1093–1110, 2002.

PIERMATTEI, D.; FLO, G.; DECAMP, C. **Brinker, Piermattei, and Flo's Handbook of Small Animal Orthopedics and Fracture Repair**. Elsevier-Saunders, 2006. 832p.

RAHN, B.A. Bone healing: histologic and physiologic concepts. In: SUMNER-SMITH, G.; FACKELMAN, G.E. (Eds.). **Bone in Clinical Orthopedics**. 2nd. ed. Stuttgart, Germany: Thieme, 2002. p. 287–300.

REEMS, M.R.; PLUHAR, G.E.; WHEELER, D.L. Ex vivo comparison of one versus two distal screws in 8 mm model 11 interlocking nails used to stabilize canine distal femoral fractures. **Veterinary Surgery**, v. 35, n. 2, p. 161–167, 2006.

ROE, S. C. Biomechanical basis of bone fracture and fracture repair. In: COUGHLAN, A. R., MILLER, A. (Ed.). **BSAVA Manual of Small Animal Fracture Repair and Management**. 1st. ed. United Kingdom: British Small Animal Veterinary Association, 1998. p. 17–29.

SAKA, G.; SAGLAM, N.; KURTULMUŞ, T.; AVCI, C.C.; AKPINAR, F.; KOVACI, H.; CELIK, A. New interlocking intramedullary radius and ulna nails for treating forearm diaphyseal fractures in adults: A retrospective study. **Injury**, v. 45, p. 16–23, 2014.

SCHANDELMAIER, P.; FAROUK, O.; KRETTEK, C.; REIMERS, N.; MANNß, J.; TSCHERNE, H. Biomechanics of femoral interlocking nails. **Injury**, v. 31, n. 6, p. 437–443, 2000.

SCHATZKER, J. AO philosophy and principles. In: JOHNSON, A. L.; HOULTON, J. E. F.; VANNINI, R. (Eds.). **AO Principles of Fracture Management in the Dog and Cat**. Stuttgart, Germany: Thieme, 2005. p. xv–xix.

SCOTTI, S.; KLEIN, A.; PINK, J.; HIDALGO, A.; MOISSONNIER, P.; FAYOLLE, P. Retrograde placement of a novel 3.5 mm titanium interlocking nail for supracondylar and diaphyseal femoral fractures in cats. **Veterinary and Comparative Orthopaedics and Traumatology**, v. 20, n. 3, p. 211–8, 2007.

SHARIR, A.; BARAK, M. M.; SHAHAR, R. Whole bone mechanics and mechanical testing. **Veterinary Journal**, v. 177, n. 1, p. 8–17, 2008.

STIFFLER, K.S. Internal fracture fixation. **Clinical Techniques in Small Animal Practice**, v. 19, n. 3, p. 105–113, 2004.

TURNER, C.H.; BURR, D.B. Basic biomechanical measurements of bone: a tutorial. **Bone**, v. 14, n. 4, p. 595–608, 1993.

VON PFEIL, D.J.F.; DÉJARDIN, L.M.; DECAMP, C.E.; MEYER, E.G., LANSLOWNE, J.L., WEERTS, R.J.H.; HAUT, R.C. In vitro biomechanical comparison of a plate-rod combination-construct and an interlocking nail-construct for experimentally induced gap fractures in canine tibiae. **American Journal of Veterinary Research**, v. 66, n. 9, p. 1536–1543, 2005.

WHITEHAIR, J.G.; VASSEUR, P.B. Fractures of the Femur. **Veterinary Clinics of North America: Small Animal Practice**, v. 22, n. 1, p. 149–159, 1992.

YAMAJI, T.; ANDO, K.; WOLF, S.; AUGAT, P.; CLAES, L. The effect of micromovement on callus formation. **Journal of Orthopaedic Science**, v. 6, n. 6, p. 571–575, 2001.

ZIOUPOS, P.; CURREY, J.D.; HAMER, A.J. The role of collagen in the declining mechanical properties of aging human cortical bone. **Journal of Biomedical Materials Research**, v. 45, n. 2, p. 108–116, 1999.